ABSTRACT

Title of thesis: CHEMICALLY FUELED TRANSIENT POROUS HYDROGELS AS AUTONOMOUS SOFT ACTUATORS

Sarangua Battumur, Master of Science, 2024

Thesis directed by: Professor Taylor J. Woehl
Department of Chemical and Biomolecular Engineering

Biomimetic materials take inspiration from biological systems to develop transformative reconfigurable synthetic materials. One example of a biological system is the contraction of muscle fibers driven by biochemical reactions. Actin filaments are crucial to cellular functions, facilitating movement, division, and structural integrity through ATP-driven polymerization and depolymerization. This ability to self-assemble and disassemble in response to biochemical signals provides a model for creating materials that mimic the sophisticated control found in biological systems.

This thesis describes the use of a chemical reaction network to rapidly and autonomously reconfigure the size of a porous polymer hydrogels within tens of minutes. This hydrogel, composed of acrylic acid and acrylamide monomers, exhibits exceptional microporosity and an ability to expand approximately 150 times its original size within 15 seconds when exposed to water. The chemical reaction network utilizes a carbodiimide molecule, which transiently converts carboxylic acid moieties to anhydride bonds, causing transient shrinking of the hydrogel. The hydrogel spontaneously swelled due to hydrolysis of the anhydride bonds. We enhance the swelling rate of the porous hydrogels by adding polymer beads loaded with formaldehyde and sulfite buffer to the reaction vessel, which generate a time delayed pH increase that accelerates the hydrolysis of the anhydride bonds. This multi-reaction network

forms porous hydrogels that contract and reswell autonomously in less than 10 minutes, compared to about 1 hour without the delayed pH change. This approach not only enables a faster reconfiguration of the porous gel induced by EDC through the hydrolysis of the anhydride due to a transient pH change, but also integrates this external stimulus into a single-step, autonomous process. This work also deepens our understanding of natural and synthetic actuation systems and how to couple different reactions to enhance their response. By harnessing the principles of bioinspired actuation, our work bridges the gap between the orchestrated movements of biological systems and the engineered behavior of synthetic materials, infusing our constructs with a level of adaptability and responsiveness that mirrors the natural world.

CHEMICALLY FUELED TRANSIENT POROUS HYDROGELS AS AUTONOMOUS SOFT ACTUATORS

by

Sarangua Battumur

Thesis submitted to the Faculty of the Graduate School of the
University of Maryland, College Park, in partial fulfillment
of the requirements for the degree of
Master of Science
2024

Advisory Committee:
Prof. Taylor J. Woehl, Department of Chemical & Biomolecular Engineering, chair
Prof. Srinivasa R. Raghavan, Department of Chemical & Biomolecular Engineering, committee member
Prof. Albertus. Paul, Department of Chemical & Biomolecular Engineering, committee member

I dedicate this thesis to my family in Mongolia—my mother, my sister, and my fiancé. Their constant support, patience, and unwavering love have been my foundation.

Acknowledgements

First and foremost, I want to extend my deepest gratitude to my advisor, Professor Taylor Woehl. He provided me the opportunity to advance my education by giving me the chance to join his group. Without his support and encouragement, I wouldn't be where I am today. I am truly grateful for your mentorship, patience, and willingness to engage in discussions and brainstorming sessions for every project I've undertaken.

To my committee members, Dr. Raghavan, who inspired curiosity in research beyond his lab, Dr. Albertus, for his support and valuable insights on my early research projects.

To Dr. Sriram, who inspired me early in my undergraduate career and gave me the opportunity to serve as a mentor in his CHBE101 program. To my graduate professors, Dr. Choi, Dr. Wang, and Dr. Chen who constantly pushed me to think beyond and helped shape my understanding of what it means to be a chemical engineering student.

To my fellow lab members, Dr. Satyam Srivastava, Yuhang Wang, Jiayue Sun, Amy Chen, Martin Ahn, Jemma Wood, and Shakti Arumugam. Dr. Satyam Srivastava, thank you for your companionship in the lab and our small conversations. Yuhang, I will miss our friendly greetings and collaborative efforts in ordering chemicals. Each of you has contributed to making my time in the lab immensely enjoyable. To Dr. Medha Rath, for her guidance and support in the beginning of my research. Additionally, I want to extend my appreciation to my undergraduate students Jemma Wood for her dedication and contributions to our work.

To my friends Paula Montero Atienza, Sam Grasso, Morine Nader, Wei-Yi Chu, Ireen Philip, Faraz Burni, Mahima Srivastava, and Funke Okunrinboye. Thank you all for making this journey an exciting, emotional, and beautiful experience.

Finally, I want to express my gratitude to my mother, who has bestowed upon me the world and countless opportunities, along with the sacrifices she has made for me. To my sister, whose presence inspires me to strive for the best version of myself and fills my life with unparalleled joy. And to my fiancé, whose unwavering love and support uplift me every day. Thank you all for molding me into the individual I am today, not just academically, but as a whole person.

Table of Contents

List of Figures

Figure 3.1. Synthesis of hybrid gel. Hybrid gel with dual responsive characteristic as shown with differing monomer ratios (left being 3:1 and right being 1:1).

Chapter 1: Introduction

1.1 Out of Equilibrium Biological Structures

Biomimetic materials take inspiration from cells to develop transformative reconfigurable synthetic materials. Cells inherently form dynamic structures like microtubules through chemically fueled dissipative assembly[1]. Within cells, reaction networks control the rates of assembly and disassembly of proteins to create transient structures[2]. For instance, guanosine triphosphate (GTP) binds to tubulin dimers, promoting polymerization, while slow hydrolysis of these complexes leads to depolymerization[3]. These mechanisms allow for rapid reconfigurations of microtubules, crucial for functions like cargo transport[4], cellular reshaping[5], and division[6].

Complex out-of-equilibrium systems like those found in cells as shown in Figure 1.1A are widespread in nature[7]. Through constant, chemically fueled input these systems can function autonomously. Examples of such systems include the dynamic assembly and disassembly of microtubules shown in Figure 1.1B. In a typical dissipative assembly cycle, non-reacting entities initially exist in a stable solution in thermodynamic equilibrium. Upon exposure to a chemical fuel, they transition into an "activated state", prompting responses such as biomolecule assembly. This activation reaction proceeds rapidly until all the chemical fuel is depleted.

Subsequently, a slower reverse reaction occurs, leading to the deactivation of the building blocks back to their initial state. This process generates transient assembled structures, with both activation and deactivation processes happening simultaneously. Eventually, dissipation of the

chemical energy causes the system to return to its original state[8].

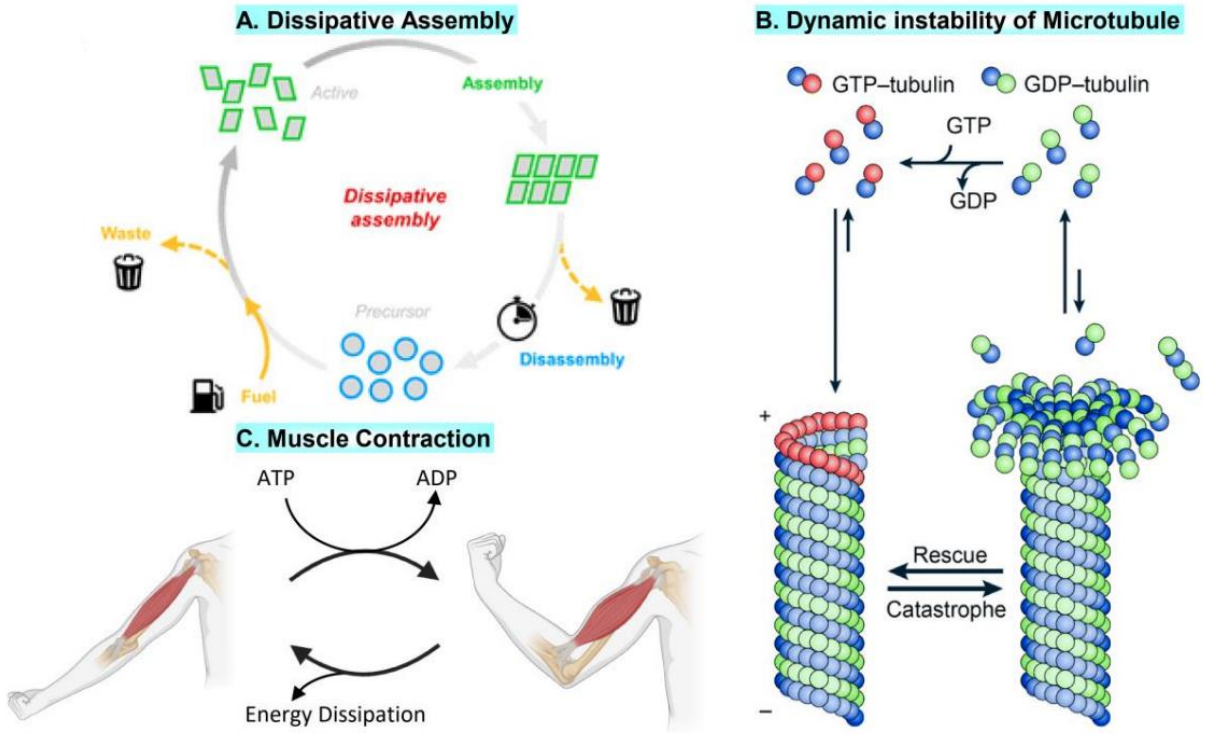

Figure 1.1. Nature Inspired chemical fuel mediated CRNs. (A) An exemplary reaction cycle involving dissipative assembly. (B) The spontaneous formation and breakdown of (C) Muscle actuation driven by the utilization of ATP.

Similarly, actin filaments are fundamental to the architecture and dynamics of cellular cytoskeletons[9], facilitating movement, division, and structural integrity through ATP-fueled polymerization and depolymerization[10]. This autonomous regulation, governed by non-equilibrium chemical reaction networks (CRNs), allows for dynamic restructuring to biochemical cues[11]. The capability of self-assembling and disassembling in response to biochemical cues offers valuable insight into the fundamentals of soft materials like hydrogels. These materials can replicate or mimic the intricate control found in biological systems, akin to the role of actin filaments in regulating muscle contraction in Figure 1.1C.

In muscle contraction, actin filaments interact with myosin to form cross-bridges essential for contraction[12]. The cycle starts with ATP binding to myosin, causing detachment from actin. ATP hydrolysis then induces a conformational change in myosin, which rebinds to actin at a new position. This sequence drives the power stroke that pulls the actin filament towards the sarcomere's center, resulting in muscle fiber shortening. Subsequently, just as muscle fibers relax and elongate when the stimulus ceases, our hydrogel autonomously expands, reabsorbing water to nearly its original size. This remarkable similarity in function between the actin-myosin complex's mechanical movements and the hydrogel's response to chemically fueled stimuli underscores the potential of our material to replicate the dynamic restructuring of biological systems autonomously.

This bioinspired approach is visually and conceptually captured in Figure 1.2, where we present our porous gel's ability to undergo similar contraction and expansion in Figure 1.2B.

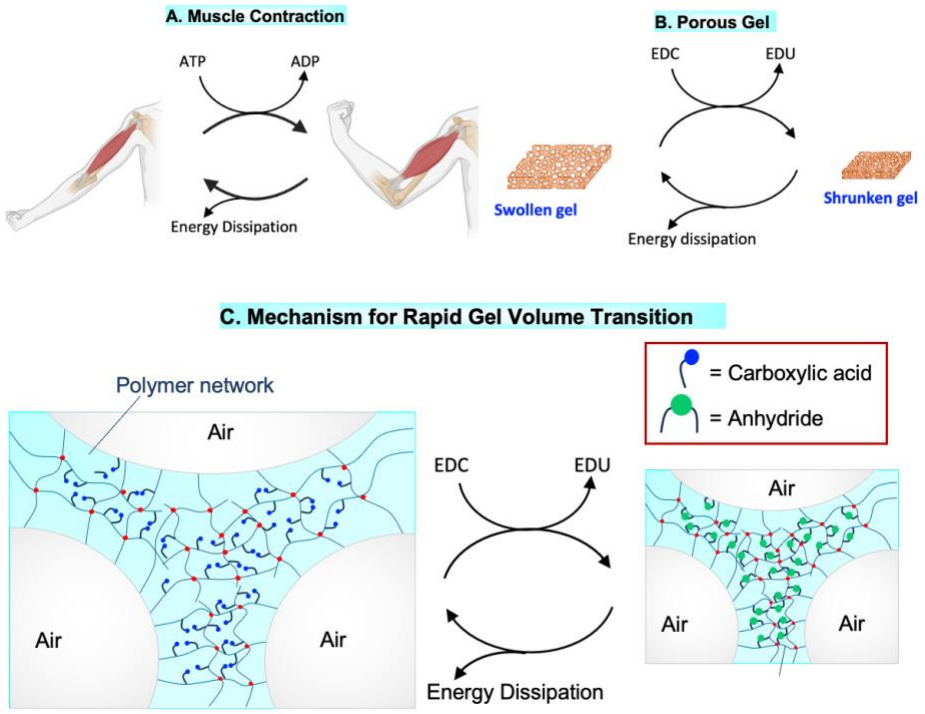

Figure 1.2. Chemical fuel mediated CRNs. (A) Spontaneous muscle actuation by consumption of ATP. (B) Contraction-expansion cycle of porous hydrogels driven by carbodiimide chemistry. (C) Mechanism for Rapid Volume Expansion.

Mimicking the cyclic interaction of actin and myosin, the porous hydrogel we have developed exhibits volumetric changes as shown in Figure 1.2C. Upon exposure to a chemical stimulus, akin to the ATP in muscle fibers, the hydrogel contracts, expelling water and reducing its volume substantially, analogous to the muscle fiber shortening during contraction.

1.2 Polymer Porous Hydrogel

A hydrogel consists of a three-dimensional network of crosslinked polymer that retains a large amount of solvent (~75 wt%) in the network[13]. The swelling ability of hydrogels is due to hydrophilic functional groups within the structure, while the crosslinks prevent them from dissolving in water. In recent years, hydrogels have become highly regarded for their ability to react to various external stimuli, including changes in temperature, pH, light, electrical fields, and different solvents[14]. One responsive behavior of hydrogels is a volumetric phase change, where the hydrogel undergoes a significant size reduction by expelling solvent in response to changes in pH, temperature, or solvent[15].

The stimuli responses of hydrogels has led to their use in a wide array of fields such as agriculture[16], drug delivery, biomedical applications[17], soft robotics, cosmetics, and others. Typically, the mesh size of hydrogels ranges from 5 to 100 nanometers. This size allows them to be permeable to small molecules like dyes or drugs, yet impermeable to larger particles such as nanoparticles or macromolecules. Synthetic hydrogels are typically created using free radical polymerization, a process initiated either by ultraviolet (UV) light or heat. In this method, the polymer chains are crosslinked through covalent bonds[18].

When a macroscale dry gel is introduced to water, it takes approximately 24 hours to reach its equilibrium size due to the slow diffusion of water into the gel. This diffusion is characterized by the formula $\tau = l^2/6D$, where τ is the timescale for diffusion, l is the length scale of the gel, and D is the diffusivity of water. Therefore, a gel with a macroscale length of about 1 cm swells over several hours. In contrast, microbeads with a much smaller size (about 10 μm) swell significantly faster, with the process taking just seconds[18].

Introducing porosity into a macroscopic hydrogel can accelerate the swelling process. By making the gel porous, the critical length scale for diffusion shifts from the overall size of the gel to the diameter of the pores. If these pores are microscale and interconnected, the swelling rates of porous gels can be 100 to 1000 times faster than those of nonporous gels.

1.3 Alternative Approaches to Hydrogel Reconfiguration

The development of stimuli-responsive hydrogels presents a transformative approach for creating adaptive, intelligent materials suited for a range of advanced applications. These hydrogels are engineered to undergo reversible transformations in response to environmental stimuli such as pH[19], temperature, light[20], and radiation[21], enabling them to meet specific, user-defined conditions. For instance, photo-controlled metallopolymer adhesives facilitate the reversible assembly of hydrogels, allowing for the dynamic reconfiguration of structures with light and heat[22]. Similarly, pH-sensitive hydrogels leverage dynamic covalent chemistry to adjust their mechanical properties in response to environmental acidity[23], whereas thermo-responsive hydrogels utilize materials with critical solution temperatures to achieve reversible phase transitions triggered by temperature changes[24].

The integration of such responsive behaviors is particularly pivotal in biomedical applications, ranging from smart drug delivery systems that release therapeutics at controlled rates and locations to soft robotics capable of navigating complex, variable environments.

1.4 Carbodiimide Chemistry

Carbodiimide chemistry, particularly with 1-Ethyl-3-(3-dimethylaminopropyl) carbodiimide (EDC), has been utilized to facilitate dynamic, responsive behavior in hydrogels. The process begins with EDC activating carboxylic acid groups on a polymer hydrogel network, transforming them into metastable anhydrides and temporarily rendering the molecule hydrophobic[25]. This induced hydrophobicity is key to driving volume phase transitions within hydrogel matrices, which can lead to the materials' swelling or shrinking in response to external stimuli.

As the system operates on a fuel-driven mechanism, the role of EDC is inherently temporary; it is gradually consumed through hydrolysis. Consequently, the anhydride groups forms are transient and revert to hydrophilic carboxylic acids upon hydrolysis. This reversion is the turning point that enables the hydrogel to resume its original swollen state, thus completing an autonomous reversible cycle of contraction and expansion.

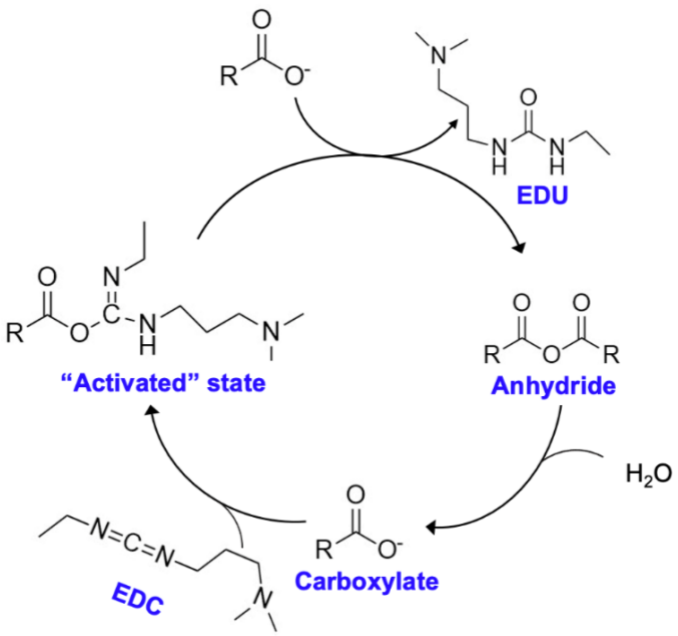

Figure 1.3. Reaction mechanism in an EDC-mediated dissipative reaction cycle.

Such a reversible swelling-shrinking behavior has far-reaching implications for the functionality of hydrogels. It allows for precise temporal control over the mechanical properties of the gel, enabling applications that require materials to adapt their shape, porosity, or stiffness dynamically. Furthermore, EDC chemistry has facilitated the development of self-assembling materials that can autonomously transition into microgels or form vesicles, depending on the configuration of the block co-polymers involved[26]. This level of control and reversibility makes EDC an invaluable component in the engineering of advanced materials for biomedical applications, smart drug delivery systems, and the burgeoning field of soft robotics.

1.5 Reconfiguration of Acrylic Acid Hydrogels in Presence of EDC

Previous studies have demonstrated that gels made of acrylic acid (AAc) exhibit significant reconfiguration in the presence of EDC. The reconfiguration time is a critical parameter for the practical application of these gels. The lifetime of these gels, defined as the period over which they reconfigure, has been measured in several studies. For instance, one set

of results showed a reconfiguration lifetime of around 7 hours[27], while another indicated a longer span of 20 to 30 hours[28]. A third study reported lifetimes varying between 8 to 17 hours, highlighting the variability and long response times observed in EDC fueled phase changes in hydrogels[29].

A key question in the field is how to overcome the typically long response times observed in hydrogels. Long response times can limit the practical utility of the gels, as rapid changes in the environment where they are applied may require quicker adaptation. Another central concern is understanding the fundamental causes behind these long lifetimes. Factors contributing to the response times and longevity of these gels could include the crosslinking density, the affinity of the polymer chains for the crosslinking agent, the degree of porosity, and the overall network structure of the polymer gel.

1.6 Mechanism of Transient pH Clock Reaction

pH plays a critical role in the chemical reactions that lead to reconfiguration of hydrogels in response to EDC. Both EDC and anhydride bond hydrolysis are catalyzed by protons and hydroxyl ions, suggesting pH changes could be utilized to enhance the response time. pH clock reactions are a potentially useful tool to induce time delayed pH changes in hydrogels. For instance, in the formaldehyde-sulfite pH clock reaction formaldehyde binds sulfite and bisulfite ions to form hydroxymethanesulfonate (HMS), which has a large pKa value of ~10 and raises the solution pH *via* protonation reactions[29]. This reaction causes a rapid pH increase from acidic to alkaline, driven by the depletion of an internal sulfite-bisulfite buffer as it is consumed by formaldehyde. The primary rate-determining step involves the dehydration of methylene glycol, while the overall pH is modulated by the internal bisulfite-sulfite buffer. Additionally, the concentration of formaldehyde influences the reaction induction period, where a lower

concentration increases the delay time. By integrating this pH clock reaction with the EDC reaction cycle, we hypothesis we can achieve precise control over the timing of hydrogel contraction and expansion. For instance, adjusting the pH clock induction period to about 5 minutes allows the pH clock reaction to activate just as the hydrogel undergoes the volumetric phase transition, facilitating rapid and autonomous reswelling. This strategic use of the formaldehyde-sulfite reaction as a pH clock introduces a novel approach for enhancing control of dynamic soft matter systems with chemical networks.

1.7 Goal and outline of thesis

This thesis explores the fundamental principles of chemically fueled dissipative assembly as a mechanism for the dynamic restructuring of biological systems and the synthetic replication of these processes in smart materials. It addresses the challenges and overcomes 1) the slow response time of hydrogels, and 2) autonomizing the external stimulus, such as pH changes, in the reconfiguration cycle of porous gels.

Our study utilizes a chemical reaction network to rapidly and autonomously reconfigure the size of a porous polymer hydrogel in a manner similar to actin filaments in muscle fibers. This hydrogel, composed of acrylic acid and acrylamide monomers, exhibits porosity and an ability to expand approximately 150 times its original size within 15 seconds when exposed to water. We enhance the chemically fueled reconfiguration rate of the porous hydrogels by adding polymer beads loaded with formaldehyde and sulfite buffer, which generate a time delayed pH increase that accelerates the reconfiguration time of the hydrogel to less than 10 minutes compared to about 1 hour without the pH change. This approach not only enables a faster reconfiguration of the porous gel induced by EDC through the hydrolysis of the anhydride due to a transient pH change, but also integrates this external stimulus into a single-step, autonomous

process. This work also deepens our understanding of natural and synthetic actuation systems and how to couple different reactions to enhance their response. By harnessing the principles of bioinspired actuation, our work bridges the gap between the orchestrated movements of biological systems and the engineered behavior of synthetic materials, infusing our constructs with a level of adaptability and responsiveness that mirrors the natural world.

Chapter 2 Chemically Fueled Transient Porous Hydrogels

2.1 Overview

Biomimetic materials represent a promising avenue for advancing synthetic materials, drawing inspiration from the intricate dynamics of biological systems. At the forefront of this exploration lies the study of actin filaments, essential components of cellular cytoskeletons[30]. Actin filaments exhibit a remarkable capacity for self-assembly and disassembly, orchestrated by ATP-fueled polymerization and depolymerization processes[31]. This dynamic behavior serves various cellular functions, including movement, division, and structural integrity, exemplifying the control mechanisms operating within living organisms.

Central to the study of biomimetic materials is the emulation of biological processes, such as muscle contraction, where actin filaments play a central role. The interaction between actin filaments and myosin, facilitated by ATP hydrolysis, drives the contraction-relaxation cycle essential for muscle function[32]. This intricate interplay, characterized by rapid, controlled assembly and motor-driven motion, serves as a blueprint for designing synthetic materials capable of autonomous action and responsiveness.

In pursuit of this biomimetic design, researchers have developed porous polymer hydrogels that mimic the dynamic behavior of muscle fibers powered by actin-myosin interactions. These hydrogels exhibit rapid, reversible contraction-expansion cycles under the influence of chemical fuels, such as carbodiimide chemistry and a pH clock reaction. Comprising acrylic acid and acrylamide monomers, these gels feature significant microporosity and dynamic crosslinking facilitated by EDC.

The contraction-expansion mechanism of the hydrogel closely mirrors the dynamic nature of muscle tissues, propelled by synchronized chemical reactions. Upon the addition of EDC, carboxylic acid groups undergo transformation into metastable configurations, inducing contraction. Concurrently, the pH clock reaction orchestrates a rapid reswelling phase, ensuring swift reversibility akin to muscle fibers returning to their resting state. Through meticulous calibration, the hydrogel transitions from its contracted to fully expanded form in minutes, echoing the rapid responsiveness observed in biological systems and most importantly overcoming the long responsive time compared to other works. This chapter will streamline the reconfiguration of the porous gel into a single-step process, achieving a quicker re-swelling within the existing timeframe and automating the accelerated reconfiguration.

2.2 Experimental Section

Materials

The chemicals used in this study include the monomers acrylamide (AAm) and acrylic acid (AAc), the cross-linker Polyethylene glycol diacrylate (PEGDA), the photo initiator, identified as lithium acylphosphinate (LAP), sodium carbonate (Na_2CO_3), polyvinyl alcohol (PVA), Tween 80, 1-ethyl-3-(3-dimethylaminopropyl) carbodiimide (EDC), MES monohydrate, formalin 37 wt%, sodium metabisulfite, sodium sulfite, calcium chloride, and alginate. All chemicals were obtained from Sigma- Aldrich.

Double-Barreled Syringe (DBS) Preparation

We utilized the method developed by Choudhary *et al.* for the preparation of the porous gels, utilizing a Double-Barreled Syringe (DBS) obtained from J Dedoes Inc[18]. The DBS, with a capacity of 3 mL per barrel, was equipped with a mixing tip of 3 mm × 16 element dimension designed to ensure homogeneous mixing of the components. One barrel was filled with a

solution containing the monomers 3:4 proportion of AAc:AAM, increasing the proportion of AAc relative to AAm in a monomer solution enhances the foaminess and consequently improves the porosity of the resulting material. Predominantly, a higher ratio of AAm tends to simply yield a hydrogel, along with a crosslinker, PEGDA, PVA dissolved in 4 wt % water, the stabilizer, Tween 80, and crosslinker. While the other barrel was composed of a solution 0.1 wt % LAP and Na2CO3 (dissolved to 20 wt % in water). This formulation of the base was selected to optimize the volume of the foam. Aluminum foil was used to cover the DBS to protect the photo initiator from degradation before polymerization.

Synthesis of Porous Gels

The synthesis process began with the extrusion of foam from the DBS into a standard Ziploc bag punched with holes from a syringe needle. Uniform distribution of the foam was achieved within the container, targeting a thickness of 0.5 – 1 cm by pushing down on the foam inside the bag with flat glass plate. Subsequent exposure to UV light for 2 minutes initiated the polymerization of the monomers, transforming the foam into a porous gel. The gel was then subjected to a water bath to eliminate residual monomers, followed by ethanol immersion to replace the water content, and finally, overnight ambient drying to yield a solvent-free porous structure. Most of the gels were subjected to drying in ethanol and glycerol for two hours before the overnight ambient drying to allow for flexible or brittle gels.

Formaldehyde - Sulfite Clock Reaction

We utilized a prior reaction protocol for the formaldehyde-sulfite pH clock reaction[29]. A 10 mL solution of 1.2 M formalin was prepared in a 40 mL beaker. Additionally, 0.2 M sodium metabisulfite and 0.02 M sodium sulfite solutions were prepared in 5 mL volumes each. The 1.2 M formalin in 10 mL was combined with the 10ml sulfite buffer mixture. The solution

(formalin-sulfite) was then combined to initiate a clock reaction before being introduced to the porous hydrogel system – 5 minutes after EDC addition. To monitor pH shifts, phenol red dye was employed as an indicator, revealing a change from about 6 to 10.2 within 20 seconds of the mixing. The pH clock reaction was modified from the original protocol by changing the concentration of formalin to be 3.6>1.2>0.6>0.1M.

Synthesis of alginate capsules

We utilized a procedure from Rath, M. et al to synthesize alginate capsules. A feed solution consisting of 2.0 wt % alginate in deionized (DI) water was prepared. This solution was loaded into a syringe and expelled through a 22-gauge needle into a reservoir containing 1.5 wt % CaCl2 solution in DI water. This process transformed the droplets into capsules with a liquid alginate core and an alginate shell, each measuring approximately 5 mm in diameter. Subsequently, the capsules were immersed separately in formalin and sulfite buffer solutions for 30 minutes with stirring. This resulted in collapsed capsules containing diffused components of the clock reaction.

Synthesis of Hybrid Porous Gels

The synthesis process was adapted by spraying two different foams side by side, allowing them to meet at an interface. This was done using a specialized dual-barrel sprayer (DBS), each barrel loaded with a different foam composition. The foams were extruded simultaneously next to each other and merged at the interface to form a hybrid gel. To distinguish between the different monomer compositions in the hybrid gel, dyes were incorporated into each foam component. The entire structure was then uniformly spread to achieve a target thickness of 0.5 – 1 cm, using a flat glass plate to press down on the hybrid foam. This was followed by exposing the material to UV light for 2 minutes to initiate the polymerization of the monomers, converting

the hybrid foam into a porous gel. The gel subsequently underwent a water bath to remove residual monomers, followed by immersion in ethanol to replace the water, and finally, it was left to dry overnight at ambient conditions to achieve a solvent-free porous structure. To modify the mechanical properties, some of the gels were subjected to a two-hour drying process in a mixture of ethanol and glycerol before the overnight ambient drying, resulting in either flexible or brittle gels.

Porous Gel Response Studies with EDC

A monomer mixture ratio of 3:1 AAc:Aam with 4 wt% PEGDA as the crosslinker was used to formulate the porous hydrogels for EDC reactions. We incubated the gels in 25 mL of MES buffer with a pH of 5.0 until they reached their equilibrium state of swelling. EDC was dissolved at 1 equivalence concentration in 2 mL of MES buffer and 2 mL added directly on top of the gel. The shape change of the porous hydrogel after addition of EDC was documented using a camcorder in time-lapsed imaging mode with images acquired every 60 seconds. Five minutes were allotted to ensure maximum shrinking, after which the clock reaction, encapsulated to facilitate diffusion-driven hydrolysis of the anhydride, was introduced, triggering the swelling of the gels. The entire cycle of the porous gel's swelling, shrinking, and subsequent reswelling was captured on a camcorder.

2.3 Results and Discussion

2.3 Synthesis of the Porous Gel

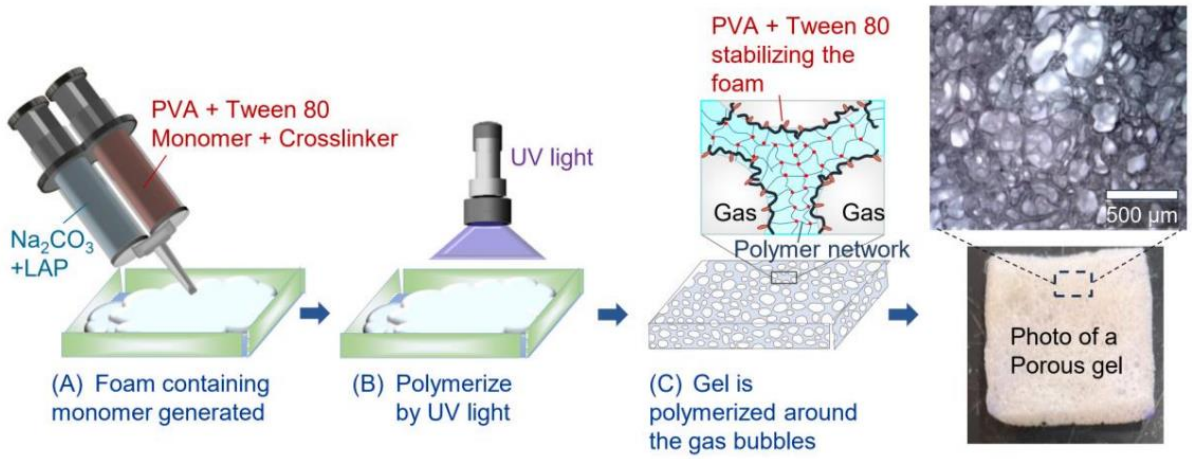

Figure 2.1. Synthesis of Porous Hydrogel. (A) Monomer solutions are placed in double-barreled syringe (DBS) before being foamed. One barrel of the DBS is acidic, solution of monomers, cross-linkers, and the PVA + Tween 80 stabilizer, while the other barrel is a basic solution with LAP. CO2 gas is produced at the mixing tip of the DBS and foam is produced. (B) The foam is polymerized by UV light for 2 min. (C) Due to fast polymerization, the bubbles in the foam are retained and the polymer is formed around. them. The gels are dried at room temperature to obtain a porous gel. The photo shows that the material is a robust solid with a sponge-like texture.

Figure 2.1 outlines the synthesis process of the porous hydrogel. For the creation of foam, a double barrel syringe was employed with one barrel for acidic components and the other for basic components. The acid barrel was filled with a mixture comprising 50 wt % monomers of acrylic acid (Aac) and acrylamide (Aam) in a 3:1 ratio, 4 wt % of the crosslinker PEGDA, and a 50 wt % stabilizer solution containing 7 wt % polyvinyl alcohol (PVA) and 2 wt % Tween 80. The base barrel contained 0.1 wt% of the photo-initiator (LAP) and 20 wt % sodium carbonate (Na2CO3) dissolved in water.

Mixing the acidic and basic solutions at the DBS tip triggers a reaction that releases carbon dioxide (CO2) gas, creating a foam which allows for the porosity property of the hydrogel. This foam is stabilized by PVA and Tween 80 (Figure 2.1A) spread evenly in a Ziploc bag, and then exposed to UV light for photo-polymerization at room temperature shown in

Figure 2.1B. Within two minutes, the rapid polymerization encapsulates the gas bubbles, forming a cross-linked polymer network and preventing the foam's collapse, thus creating a porous hydrogel (Figure 2.1C). Post-polymerization, the gels are soaked in water to extract any unreacted monomers, followed by dehydration through solvent exchange with ethanol. After hardening, the gel is removed and dried at room temperature, resulting in a sponge-like solid, as depicted in Figure 2.1.

2.3.1 Chemically Fueled Reconfigurable Behavior of the Porous Gel

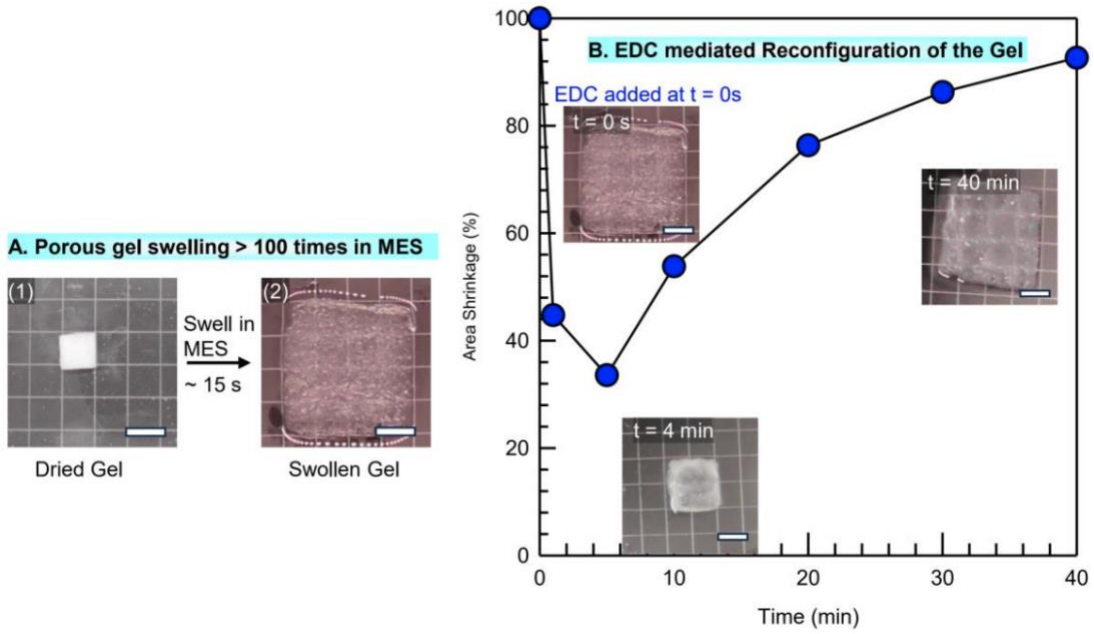

Figure 2.2. EDC driven autonomous contraction-expansion of porous gels. (A) A 1 cm x 1 cm piece of gel is swollen in MES buffer for 20 seconds. The gel swells ~ 150 times in size. (B) EDC is added at t = 0 s to the swollen gel. The gel shrinks to 30 % of its initial size in 5 mins. The gel reswells to 92 % of its size after a total of 40 mins. Scale bar: 1 cm.

In previous research, it was established that the porous hydrogels possess an approximate pore size ranging between 200-300 μm, a porosity of around 91%, and an extensive

interconnected network of pores[18]. This structure is critical for the gel's performance, particularly its hydration behavior. When a dried porous gel sample is submerged in water solution, it exhibits a remarkable expansion, swelling to more than 200 times its dry weight, with its dimensions increasing fourfold in just 15 seconds. The rapid swelling is attributed to the gel's porous microstructure, which facilitates quick water uptake through capillary action and reduces the diffusion distance into the hydrogel[18].

The inherent high porosity and the continuity of the pores endow the gel with the capability for fast volumetric changes. This is in appreciable contrast to solid hydrogels of the same chemical composition, whose swelling and contraction are hindered by the slow diffusion of water through their nano porous networks.

In our studies, experimentally a 3:1 acrylic acid - acrylamide (Aac:Aam) porous gel, crosslinked with 4 wt% poly(ethylene glycol) diacrylate (PEGDA), demonstrated significant volumetric changes upon chemical stimulation. This gel, when placed in a 20 mL 2-morpholinoethanesulfonic acid (MES) buffer at pH 5.10, swelled to approximately 15 times its original size in about 20 seconds and achieved a swelling equilibrium rapidly. The introduction of one mole of EDC equivalent to the moles of carboxylic acid in the gel, into the MES buffer initiated a drastic collapse, reducing the gel to about 50% of its swollen area within 40 seconds, and to approximately 30% within 4-5 minutes. Remarkably, the gel then spontaneously re-swelled to 92% of its original size over the following 40 minutes as shown in Figure 2.2.

The shrinkage and subsequent re-swelling of the gel are ascribed to the EDC reacting with the hydrogel's carboxylates to form non-polar, metastable anhydride bonds. These non-polar groups, being poorly soluble in the MES buffer, cause the gel to undergo a volume phase transition, resulting in the expulsion of a substantial amount of water[18]. Optical micrographs

captured these changes, showing the hydrated gel before and the dehydrated network after EDC addition. These images and accompanying schematics detail the gel's response mechanism, where the formation of anhydride bonds by neighboring carboxylate groups triggers the expulsion of water and shrinkage of the gel. This process does not allow for full recovery to the hydrogel's original dimensions, likely due to the generation of a urea byproduct from EDC hydrolysis, which increases the ionic strength of the surrounding water, thus affecting the gel's expansion capacity.

2.3.2 Effect of varying monomer ratio on porous gel reconfiguration

At the onset of our study, we initially employed a 3:1 acrylic acid (Aac) to acrylamide (Aam) monomer ratio. This specific ratio was chosen because it maximizes foam production, which in turn facilitates rapid swelling of the gels due to the increased availability of acid. To explore how the composition of porous gels affects their longevity, and the dynamics of their shrinking/swelling behavior, we varied the ratio of the ionic monomer (Aac) to the nonionic monomer (Aam) in the presence of EDC.

Throughout this experimentation, we maintained a constant monomer weight percentage at 50% in the precursor mixtures. We synthesized porous gels with varying Aac:Aam ratios, specifically 1:0, 3:1, 1:1, and 1:3, hypothesizing that gels with a higher Aac content would exhibit greater swelling compared to their nonionic counterparts. Hence, we observed the following order of swelling ratio: 1:0 > 3:1 > 1:1 > 1:3. Figure 2.3 shows the response of the swollen porous gels to EDC addition.

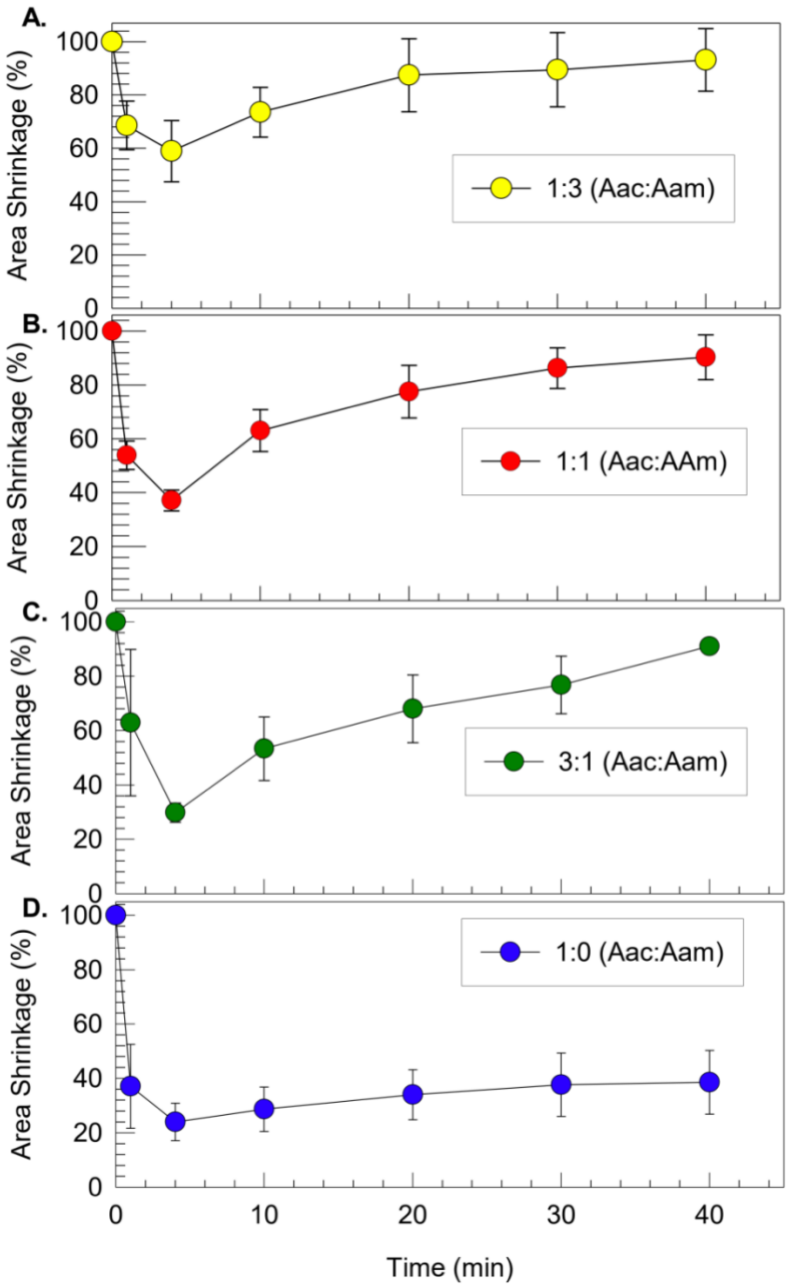

Figure 2.3. Varying monomer ratio on porous gel reconfiguration. (A) 1:3 gels show least shrinkage and fastest recovery, followed by (B) 1: 1 gels. (C) 3:1 gels show a high shrinkage (~ 30%) and recover within 40 mins. (D) 1:0 gels shrink the maximum but take hours to return to original state.

The initial gel mass was 50 mg and each gel was swollen in 25 mL of MES solution. One equiv. of EDC was added to the gels at t = 0 s and the swelling kinetics were recorded using a video camera. The time-dependent plots were generated by manually measuring the gel area at each time point using image analysis. We observed that the 1:3 porous gels contracted the least (~ 60 %) but recover the fastest with more than 90 % of the gel area recovered within the first 20 mins. The 3:1 and 1:1 gels showed similar amounts of contraction (30-40 %), with 3:1 gels shrinking slightly more than the 1:1 gel. The 1:1 gel has a faster recovery time (~90% in 30 mins) than the 3:1 gel (~ 90% in 40 mins).

This behavior among the gels can be explained by the differences in Aac concentration in each gel. Since 1:3 gel contains the least amount of Aac, it forms the lowest concentration of anhydride bonds and shrinks the least, followed by 1:1 and then 3:1.

Likewise, the concentration of anhydride being hydrolyzed back to carboxylic acids is the lowest for the 1:3 hydrogel so it requires less time for the gel to recover its size. However, to our surprise, although the 1:0 gels reached the largest % area contraction (~15-20% of the initial area) in the shortest time (~2-3 mins), the gel did not recover its initial size for 5-6 hours. Although we expect the pure Aac gels to recover the slowest due to a higher anhydride concentration, the decrease in recovery rate was not commensurate with the increased carboxylate concentration.

We hypothesize that the pores in the 100 % Aac hydrogels, which possess a high concentration of carboxylate groups, collapse due to strong hydrophobic effects and formation of high concentrations of anhydride bonds. The pore collapse limits access of water to the anhydride bonds and the hydrolysis rate is substantially diminished. Based on the findings in this

composition study, the 3:1 gel showed a combination of both high shrinkage percent and fast recovery, so it was used for subsequent experiments varying fuel concentration.

2.3.3 Effects of EDC Concentrations

Our investigation further explored the influence of varying concentrations of chemical fuel on the autonomous contraction and expansion behavior of a 3:1 (Aac:Aam) porous hydrogel. By incrementally raising the EDC concentration from 0.5 equivalents (equiv.) to 8 equiv., we examined the response kinetics of the gel, as detailed in Figure 2.4.

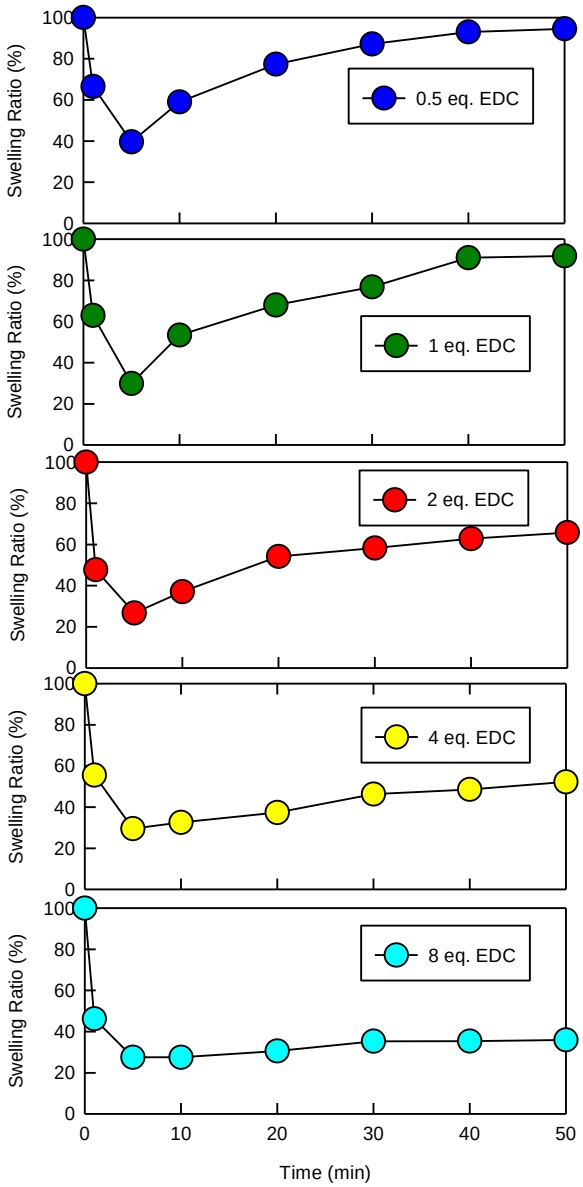

Figure 2.4. Varying concentrations of EDC on porous gel reconfiguration. A)-(E) show that increasing the EDC concentration increases the time it takes for the gel to recover.

Across all tested concentrations, the gels consistently shrank to their minimum size within approximately 5 minutes. At 0.5 equiv. of EDC, the gel diminished to about 50% of its original size in 5 minutes and subsequently re-swelled to around 90% within 40-50 minutes. In contrast, with higher EDC equivalents—1, 2, 4, and 8 equiv.—the gels contracted more significantly, reaching around 30% of their initial size in about 5 minutes. However, the time

taken to re-swell varied: 1 equiv. of EDC led to 90% recovery in 40 minutes, 2 equiv. to approximately 77% in 50 minutes, and 4 equiv. to about 55% in the same timeframe. In the case of 8 equiv. of EDC, the gel stayed at a minimum of around 25% of its starting area for about 45 minutes before slowly beginning to re-swell over several hours.

The observed trend aligns with the findings of Heckel et al.[42], who studied similar volume phase transition kinetics in poly(acrylic acid) microgels. The introduction of EDC triggers the transformation of carboxylate groups to anhydrides, which then hydrolyze overtime. With 0.5 equiv. of EDC, the gel does not shrink to the 30% level observed with higher EDC concentrations, possibly due to an insufficient conversion of carboxylates to anhydrides, as illustrated in Figure 2.4. This is attributed to the cyclic nature of the chemical reaction network, where an immediate reverse reaction from anhydrides back to carboxylic acid is observed. At this concentration, EDC is the limiting factor in the reaction.

Beyond 1 equiv. of EDC, the gels reach a quasi-steady state, maintaining their shrunken size until the fuel is entirely consumed, shown in Figures 2.4 B-D. In this state, the presence of excess EDC ensures that all carboxylates are converted to anhydrides, and the rate at which the gel contracts or expands is governed by the slower hydrolysis of anhydrides. With anhydride formation outpacing hydrolysis, the gel remains stable in its contracted state when in the presence of excess EDC. The experiments reveal that while the minimum size of contraction stabilizes beyond 1 equiv. of EDC, the overall re-swelling capability is influenced by the EDC concentration, with higher concentrations leading to prolonged contracted states.

2.3.4 Cycling of EDC on Gel Reconfiguration

Prior experiments with varying equivalents of EDC demonstrated that at 1 equivalent, the gels contracted significantly, reaching approximately 30% of their original size within 5 minutes.

Therefore, we decided to further investigate the cycling of EDC at this equivalence. The MES-EDC porous gel system underwent a three-night cycling process, wherein each day, the gel was treated with fresh 3 MES solution before introducing EDC. Following 40 minutes of the MES-EDC solution was removed from the gel system and replaced with freshly prepared MES solution for the remainder of the night. This procedure was repeated daily to ensure the gel maintained its maximum expansion potential before the introduction of EDC. The cycling of the MES-EDC reconfiguration system demonstrated the gel's reversibility and its ability to maintain consistent volume porosity even after multiple cycles of swelling and shrinking as shown in Figure 2.5.

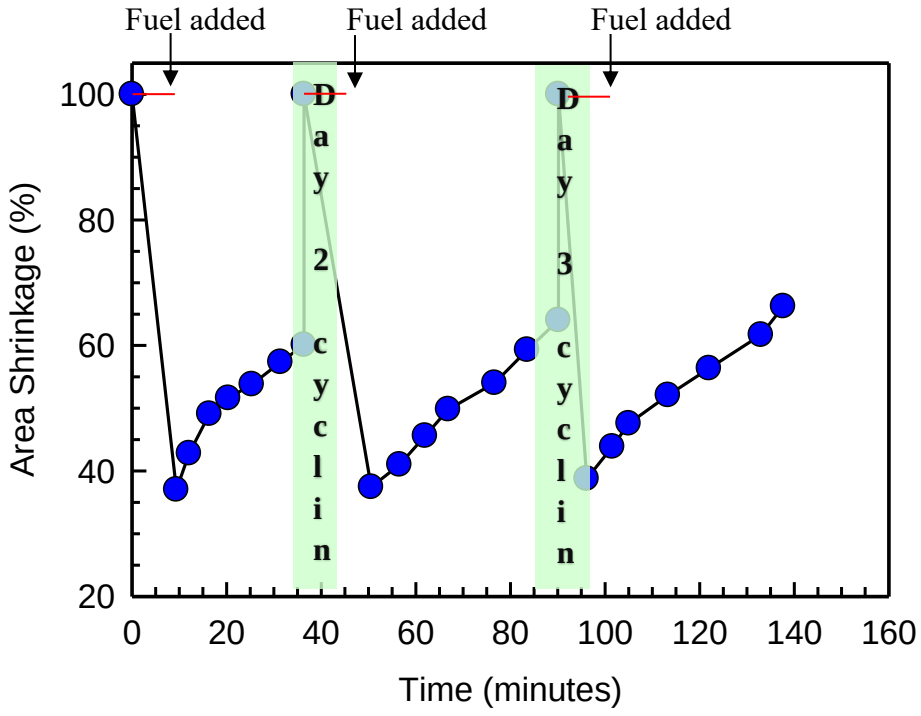

Figure 2.5. Cycling of EDC on gel reconfiguration over the duration of 3 nights. Daily, 2 mL of (MES+EDC) was added to initiate EDC-induced shrinkage, followed by immersing the gels in fresh 15 mL of MES overnight. This process was repeated each day, beginning with inducing shrinkage, documenting the re-swelling, and refreshing the MES solution.

While each successive day of cycling shows a slight decrease in shrinkage, the extent of re-swelling observed on day 3 is greater compared to the initial cycling phase. The hydrogel's ability to undergo consistent cycling without an appreciably decrease in its volume or degradation of its porous structure is crucial for ensuring reliable performance over time in various applications. An essential aspect of maintaining the gel's functionality is the control of its environment. By introducing external stimuli, we can enhance the gel's structural configuration, effectively tuning its properties for specific uses.

Our study aims to demonstrate that introducing chemically fueled inputs that can influence the gel's response behaviors, which is particularly relevant when considering the typically long response times observed in hydrogels. These extended response times could hinder the practicality of hydrogels in dynamic environments that demand rapid adaptation. Therefore, a central focus of our research is not only to improve the gel's responsiveness but also to unravel the underlying mechanisms that govern these prolonged lifetimes, which has significant implications for the development and optimization of hydrogel-based applications.

2.3.5 Effect of Strong Base in the MES-EDC Reaction Network on Gel Reconfiguration

In existing experiments, adding EDC to MES-swollen porous gels resulted in their contraction to 30% of their original size within 5 minutes post EDC introduction. These gels then spontaneously expanded to their initial size within 40-60 minutes, with variations observed across different samples of porous gels. However, the inherent reaction kinetics of EDC and its metastable intermediate, the anhydride bonds, limits the reconfiguration rate of porous gel to about 60 minutes.

To enhance the reconfiguration rate of the porous gels, we propose initiating a secondary reaction cycle that transiently changes the solution pH precisely 5 minutes following the addition

of EDC. This timing aligns at the point the hydrogel is most contracted by EDC, ensuring maximal contraction before initiating the secondary reaction.

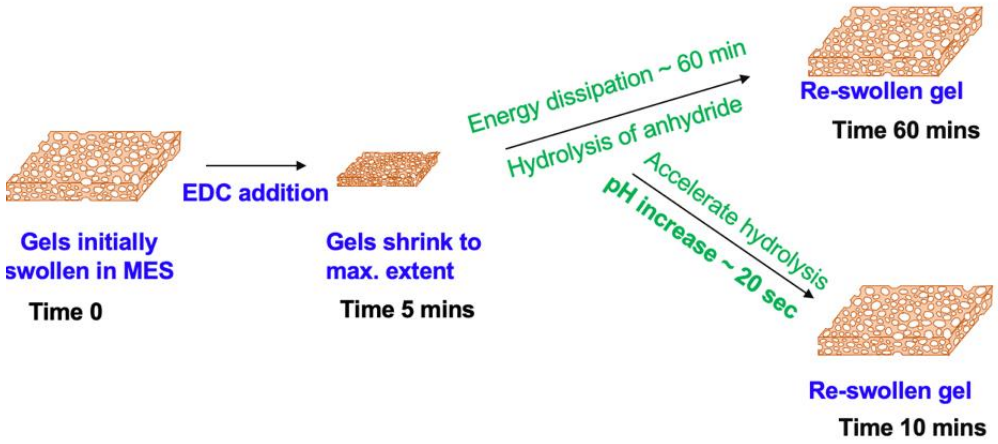

Figure 2.6. Schematic illustrating the effect of increased pH on the hydrolysis of anhydride for accelerated reconfiguration of the porous gel. By introducing a secondary pH reaction cycle, the gel can re-swell within 10 minutes, in contrast to the typical MES-EDC system where EDC energy dissipation takes up to 60 minutes.

This approach leverages the metastable yet pH-sensitive intermediate anhydride hydrolysis rate, underscoring the need for a secondary reaction to rapidly elevate the pH of the MES-EDC porous gel system. By increasing the pH of the system significantly accelerates the hydrolysis of anhydride rendering its inactive and thus facilitating a faster reconfiguration period. Given that EDC operates optimally under slightly acidic conditions and becomes inactive as the pH rises, introducing a reaction cycle that sharply increases the pH during the hydrogel's contracted phase could facilitate a more rapid expansion beyond what is achievable with the MES-EDC only reaction cycle, as evidenced in Figure 2.6.

At the 5-minute mark of maximum contraction, the pH of the MES-EDC gel system stands at 5.30. To demonstrate the effectiveness of this pH-dependent porous gel system, we introduced 0.5 M NaOH with an initial pH of 13.7 five minutes after adding EDC. Experiments

involving different concentrations of NaOH were carried out, revealing that an initial concentration of 0.5 M NaOH served as the threshold for achieving faster reconfiguration than the MES-EDC only reaction network. Any concentration below 0.5 M resulted in similar reconfiguration of the porous gel as observed with the MES-EDC-only system. The resulting pH of the MES-EDC-NaOH porous gel at the 5-minute maximum contraction was measured to be 13.2, significantly more alkaline compared to the MES-EDC porous gel system.

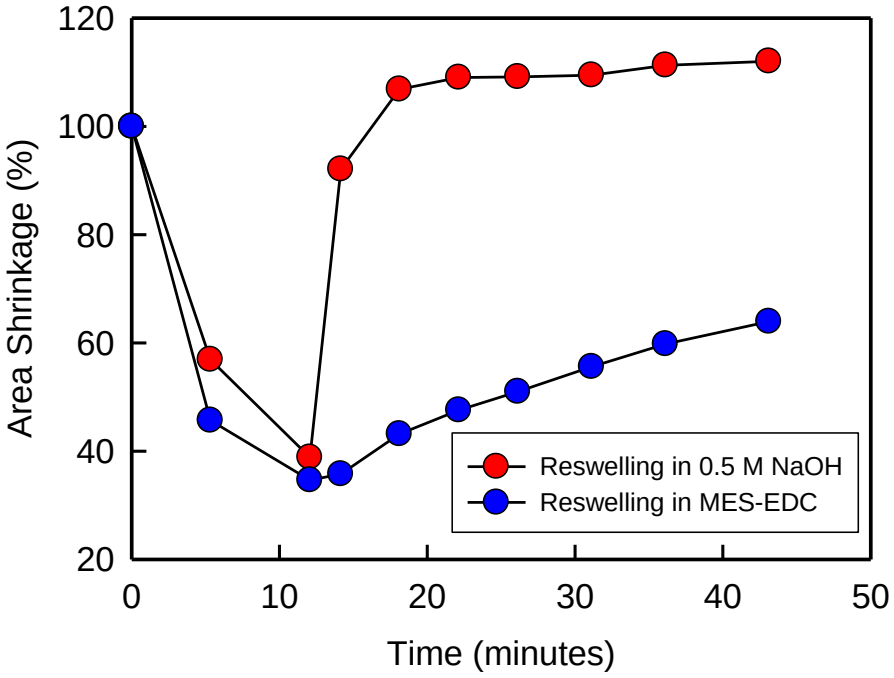

Figure 2.7. Effect of introducing a strong base secondary reaction on the pH sensitivity MES-EDC porous gel system. NaOH was added 5 minutes at the peak gel contraction.

The incorporation of a highly alkaline solution allows the porous hydrogel to expand more rapidly than is achievable with the MES-EDC-only reaction network. In Figure 2.7, not only showed a re-swelling time of less than 15 minutes—surpassing the efficiency of the MES-EDC network alone—but also revealed that the porous gel expanded beyond its initial size by an

additional 20%. This evidence strongly supports the advantage of increasing the pH to achieve more rapid anhydride hydrolysis and more rapid autonomous reswelling of the porous hydrogels.

2.3.6 Integration of the Transient pH Clock Reaction

Adding NaOH to the system requires actively intervening in the reaction cycle, making the system no longer autonomous. To retain the autonomous nature of the hydrogel shape configuration, we desire to add all the chemical 'fuels' at the zero-time point. Here we propose the formalin-sulfite clock reaction as a potential approach to achieve a time-delayed pH increase to autonomously accelerate the reconfiguration rate of porous gels. In this pH clock reaction formaldehyde reacts with bisulfite ions to form the formaldehyde-sulfite adduct, hydroxymethanesulfonate (HMS). This adduct has a high pKa of ~10, so it consumes protons and increases the solution pH to near 10.

The buffering action of HSO3- and SO3- ions initially maintains an acidic environment. As this buffer reacts with formaldehyde there is a rapid increase in pH over a time tens of seconds. For instance, for an initial formalin concentration of 1.2 M the pH rapidly increased from about 4.7 to 10.7 within just 20 seconds of mixing, as illustrated in Figure 2.8.

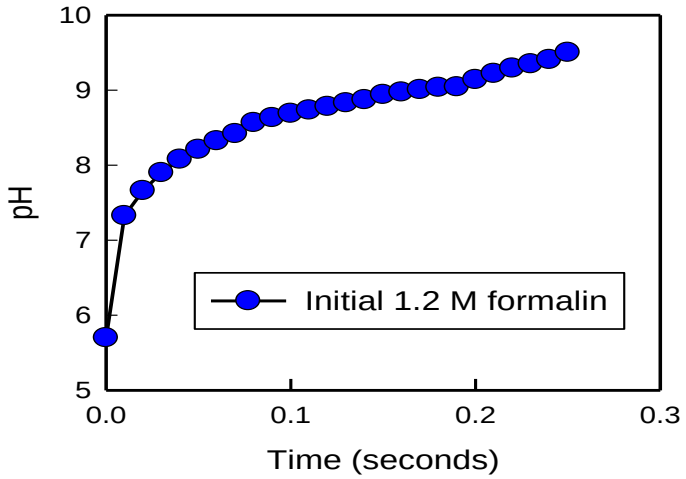

Figure 2.8. pH spike observed in the formalin-sulfite buffer clock reaction. When 1.2 M formalin is mixed with a mixture of 0.2 M sodium metabisulfite and 0.02 M sodium sulfite, the pH rapidly shifts from acidic to alkaline in less than 20 seconds.

Here the transient increase in pH is designed to enhance the hydrolysis rate of the anhydride, thereby facilitating hydrogel reswelling (Figure 2.9).

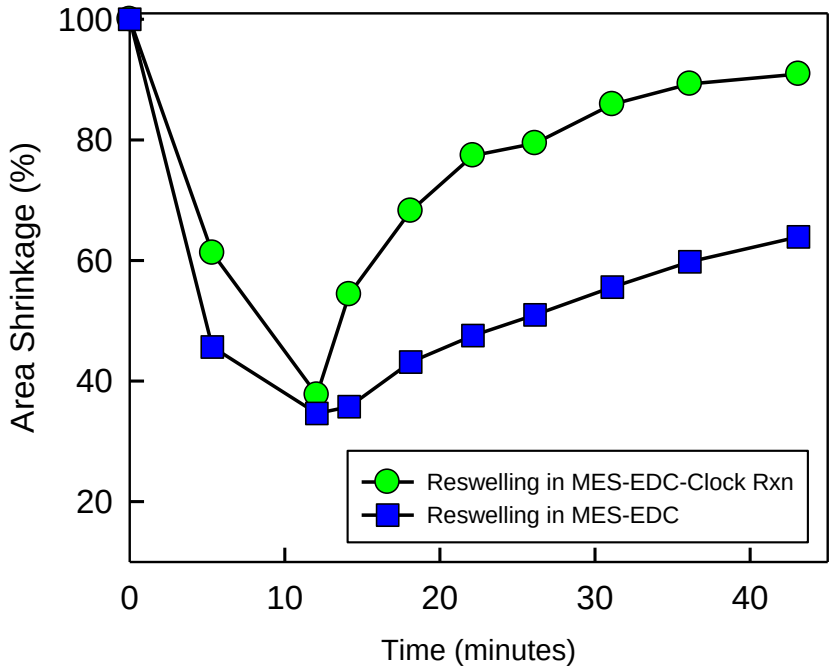

Figure 2.9. Effect of introducing a formalin-sulfite buffer clock, secondary reaction at the 5-minunte maximum contraction on the pH sensitivity MES-EDC porous gel system.

We therefore integrated the formalin-sulfite clock reaction into our existing, reconfigurable MES-EDC porous hydrogel network after observing a transient pH spike at the onset of the clock reaction. The formalin-sulfite mixture clock reaction, true to its name, involves combining formalin and sulfite mixtures.

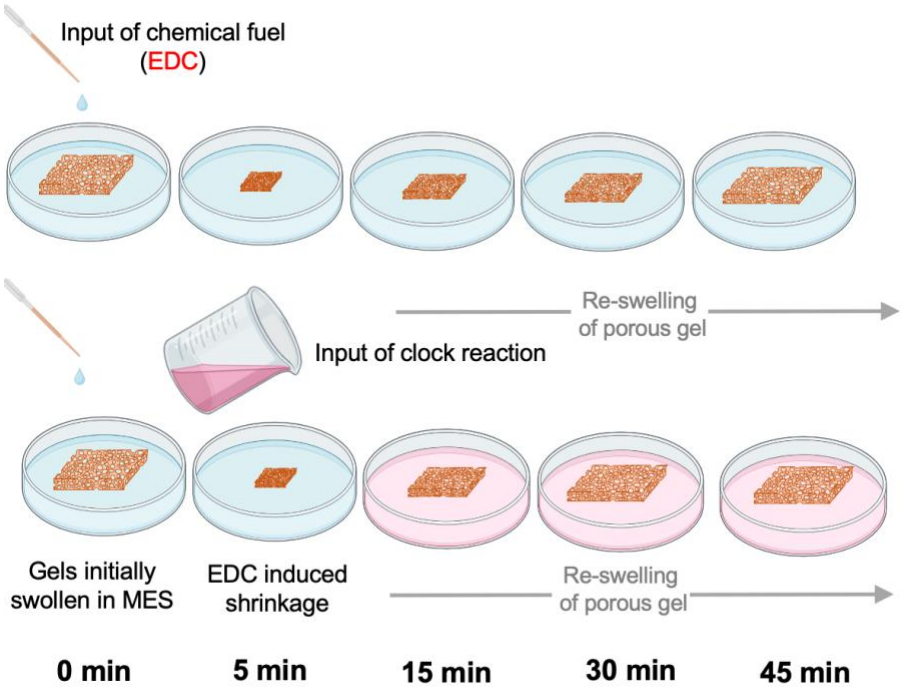

Figure 2.10. Schematic illustrating the initial setup for the MES-EDC reconfiguration, compared to the implementation of a secondary reaction cycle using the clock reaction for an even faster reconfiguration. This setup achieves maximum contraction induced by EDC within just 5 minutes.

Initially, a 1.2 M formalin solution was prepared by diluting formaldehyde in 10 mL of water. Subsequently, a sulfite buffer mixture was created by combining 0.2 M sodium metabisulfite and 0.02 M sodium sulfite in 5 mL of water each, yielding a 10 mL solution. This sulfite mixture was then mixed with the 10 mL formalin solution to produce a 20 mL final solution, which triggers the clock reaction characteristic of the formalin-sulfite interaction.

Immediately after its preparation, this mixture was introduced into a porous gel system at the peak of contraction induced by EDC, which occurs 5 minutes post EDC addition to the swollen MES porous gel in Figure 2.10.

The incorporation of the formalin-sulfite clock reaction as a secondary reaction cycle into the porous gel does not match the rate of the NaOH-induced reconfiguration; however, it is

noteworthy that 15 minutes post maximum contraction, the gels exhibited an expansion approximately 20% greater than that observed without the integration of clock reaction. The increased re-swelling is indicative of the clock reaction being affective to the porous gel as it is accelerating the hydrolysis of the anhydride therefore further allowing the porous gel to re-swell.

2.3.7 Optimal Conditions for Clock Reaction

Our initial methodology involved adjusting the timing of the pH clock reaction to activate approximately 5 minutes after introducing a mixture of EDC and formaldehyde/sulfite/bisulfite into the porous hydrogel. The idea was for the reaction to commence once the hydrogel had contracted to its minimum size, leading to a rapid increase in pH by several units in under a minute following the induction period. This method aimed to produce hydrogels capable of autonomously adjusting their size in less than 15 minutes.

To tune the induction period, we experimented with aging the formalin solution to produce different amounts of formaldehyde when mixed with the sulfite-bisulfite buffer, but this modulation did not notably change the induction time of the clock reaction. We observed similar results whether the formalin was aged for 12 hours, 6 hours, or freshly prepared, indicating that aging the formalin did not effectively influence the induction period of the clock reaction. Therefore, to optimize the reconfiguration of porous gels using the clock reaction, we instead varied the initial concentration of formalin. Formalin acts as a limiting reactant in this reaction mechanism, reacting with both sulfite and bisulfite ions to produce the HMS adduct.

We varied the initial concentrations of formalin in descending order of 3.6>1.2>0.6>0.1M prior to adding the metabisulfite-sulfite buffer. We then monitored and recorded the transient pH changes of the clock reaction over a duration of 100 seconds. Each

concentration of formalin starts with a rapid increase in pH, reaching a peak within the first few seconds. This is particularly pronounced in the higher concentrations (3.6 M and 1.2 M). After this initial spike, the pH levels off and stabilizes at a value that remains relatively constant for the remainder of the observed period as shown in Figure 2.11.

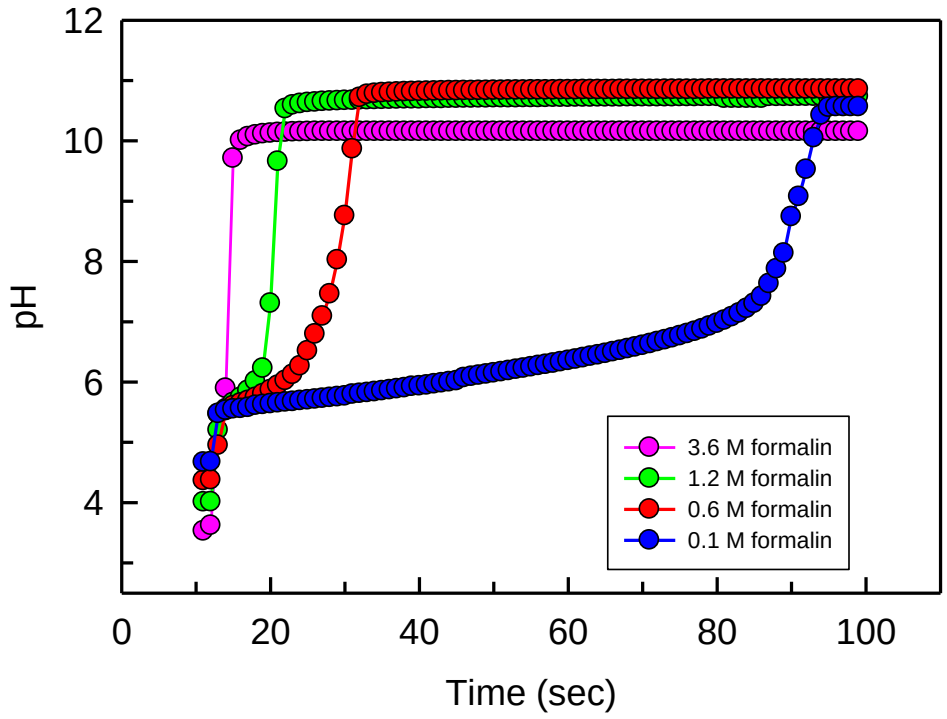

Figure 2.11. Effect of pH change in the formalin-sulfite buffer reaction with decreasing initial formalin concentrations of 3.6>1.2>0.6>0.1 M on the autonomous reconfiguration of porous hydrogel over an observed time period of 100 seconds.

The pH response to varying concentrations of formalin, when reacted with the metabisulfite-sulfite buffer, illustrates differences in the timing and magnitude of pH spikes. The highest concentration, 3.6 M formalin, shows the most immediate and pronounced increase in pH, peaking near 11 and stabilizing between 10 and 11. This rapid pH change indicates that a substantial amount of formalin reacts with the buffer, quickly overwhelming its capacity to maintain an acidic environment. Following this, the 1.2 M formalin concentration also reaches a

stabilization point between pH 10 and 11, but the initial spike is delayed by about 10 seconds compared to the 3.6 M formalin. This delay suggests a slower reaction rate or less buffer saturation.

Further down the concentration scale, the 0.6 M formalin exhibits a similar stabilization slightly higher than that of the 1.2 M formalin, but its pH spike occurs about 20 seconds later than the 3.6 M concentration. This additional delay highlights a progressively reduced rate of reaction and less impact on the buffer system as the formalin concentration decreases.

The most diluted concentration, 0.1 M formalin, displays the most gradual onset of pH change, with the spike only beginning after 90 seconds, starting from a lower initial pH and stabilizing around pH 11. This markedly delayed reaction underscores the minimal influence of low formalin concentration on the buffering capacity, allowing the buffer to maintain its acidic condition much longer before being overwhelmed.

As formalin is added and reacts to form HMS, it consumes protons (H+), leading to a significant increase in pH. This aligns with the initial pH spikes observed for each concentration of formalin. The extent and rapidity of the pH increase are proportional to the concentration of formalin. Higher concentrations result in quicker and more significant pH changes. Once the majority of the bisulfite and sulfite ions have reacted and converted into HMS, the rapid increase in pH ceases and the pH stabilizes. The stabilization occurs near pH 10, which correlates with the pKa of HMS.

2.3.8 Optimal Conditions for Clock Reaction

Figure 2.12 illustrates the effect of varying the initial concentrations of formalin in descending order of 3.6>1.2>0.6>0.1 M before adding them to the metabisulfite-sulfite buffer,

previously used in a pH experiment, to study their impact on the reconfiguration of the porous gel.

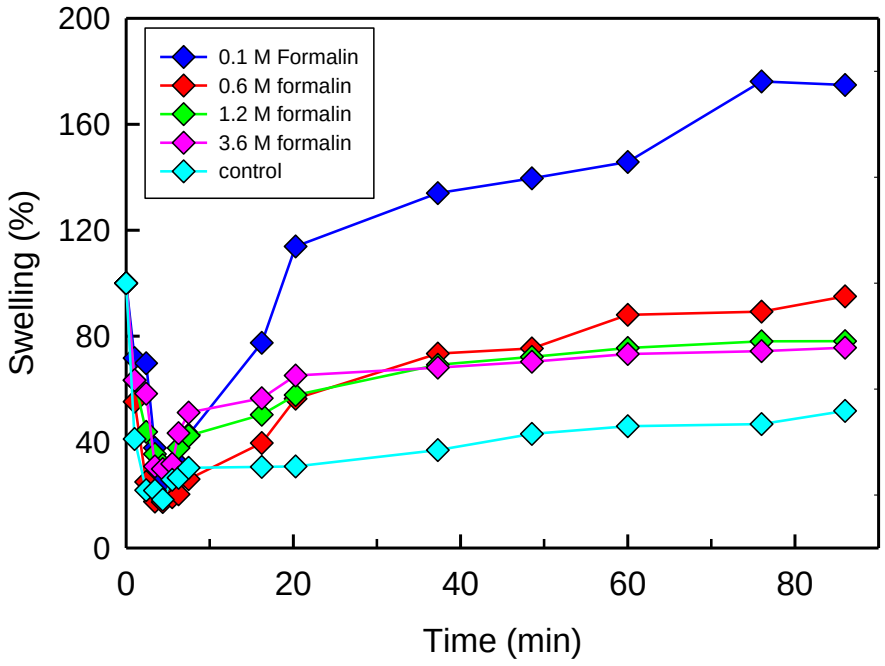

Figure 2.12. Effect of decreasing initial formalin concentrations of 3.6>1.2>0.6>0.1 M on the autonomous reconfiguration of porous hydrogel. The control being MES-EDC reaction network with no addition of secondary, clock reaction.

At, the lowest concentration of formalin, 0.1 M, the porous hydrogel exhibits the most substantial swelling, reaching up to nearly 200% after 60 minutes. At lower formalin concentrations, fewer crosslinks are formed within the hydrogel matrix, which preserves more of the carboxyl groups' functionality. These carboxyl groups are crucial for the gel's ability to absorb water, as they can undergo reactions with EDC to form non-ionic anhydride intermediates which temporarily reduce the hydrophilicity of the gel, causing it to contract/shrink.

Higher pH values can facilitate the hydrolysis of anhydride bonds that form within the gel structure. Anhydrides, which form through reactions involving carboxyl groups, are more

susceptible to hydrolysis in alkaline conditions. The breakdown of these anhydride bonds would regenerate carboxyl groups, increasing the gel's hydrophilicity and thus its ability to re-swell.

At the 0.1 M formalin concentration, where pH is higher due to less formalin-induced acid production, the environment may be more conducive to the hydrolysis of anhydride bonds. This would not only regenerate carboxyl groups but also enhance their ionization, further increasing the gel's capacity to absorb water.

With lower formalin concentrations (like 0.1 M), fewer crosslinks likely form, reducing the density of anhydride bonds compared to higher concentrations. Combined with a higher pH, this environment is ideal for rapid and extensive hydrolysis, leading to significant swelling as observed in the graph. This results in a greater extent of re-swelling because the structure is less restricted, and more groups are available to interact with water molecules.

Conversely, at higher formalin concentrations like (3.6 M), more extensive crosslinking reduces the number of free carboxyl groups available for reaction and likely increases the number of anhydride bonds. The lower pH in these samples (due to more acid formation from higher amounts of formalin) would also slow down the hydrolysis of anhydride bonds, resulting in less swelling as the rigid structure restricts water absorption.

2.3.9 Integration of One-Step, Capsule Clock Reaction

The current reconfiguration of porous gels using the MES-EDC-clock reaction reconfigures within 15 minutes—almost twice as fast as the time required for the gels to return to their original size using just the MES-EDC reaction network. However, this process remains bifurcated: initially, the gels are allowed to shrink maximally under the influence of EDC; subsequently, the clock reaction is introduced to accelerate reconfiguration, thus necessitating a two-step procedure. To streamline this into a single-step process, where both the EDC and clock

reaction are combined and administered simultaneously—yet still permitting the EDC-induced shrinkage followed by the clock reaction activation—a strategy was needed to delay the onset of the clock reaction in Figure 2.13.

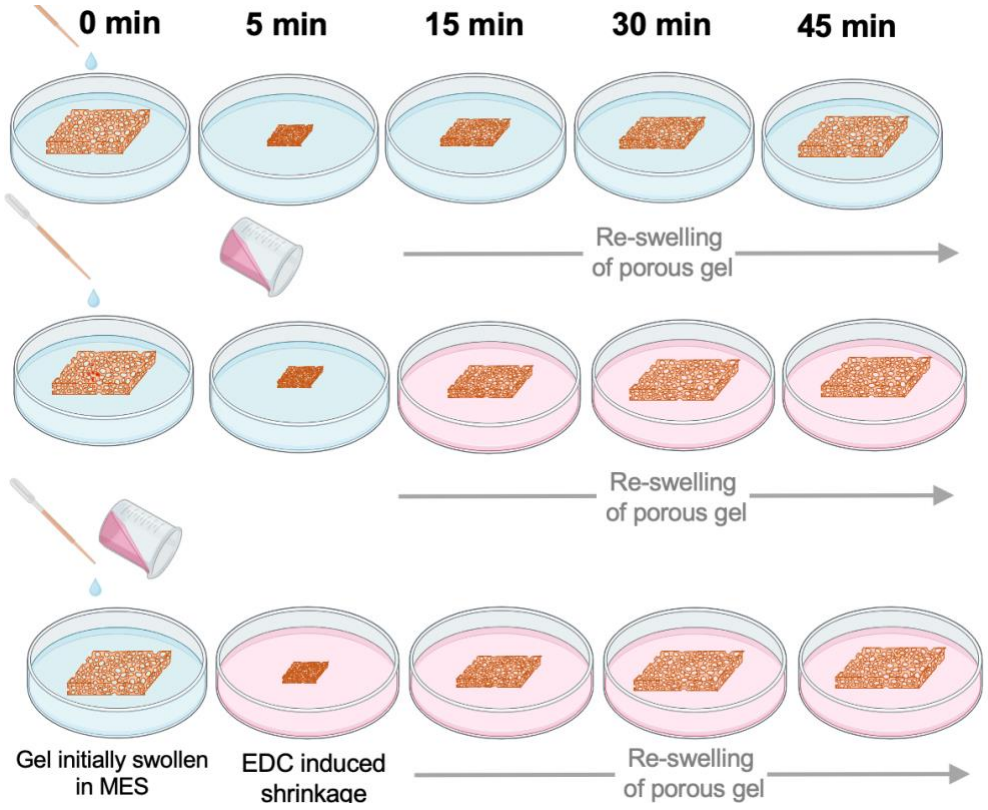

Figure 2.13. At the top, the schematic shows the MES-EDC reconfiguration setup. Below, it details the introduction of the clock reaction as a secondary reaction. Followed by the the autonomous streamlined system, which encompasses both faster and autonomous re-swelling of the porous gel.

To address this, we adapted the clock reaction by encapsulating the reactants in bead-like capsules. This method enables the clock reaction reactants to diffuse into the capsules, allowing for a controlled release into the porous gel system once added. The design of the alginate-calcium chloride bead facilitates the controlled release of the clock reaction species, ensuring compatibility with EDC. This allows EDC to effectively induce shrinking, while simultaneously triggering the clock reaction once the species diffuse out.

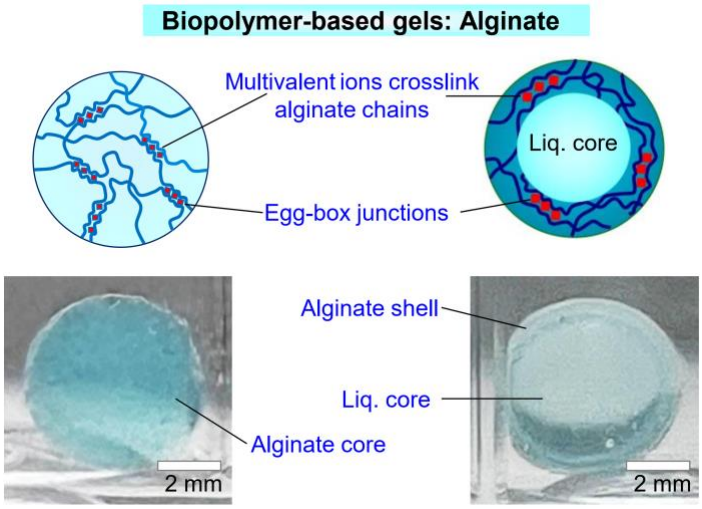

Figure 2.14. Alg capsules can be formed by dropping an Alg solution into a Cu^{2+} solution. In this case, we obtain a gelled core capsule. In the second case, a thickened $CuCl_2$ solution is dropped into an alg solution. In this case, we obtain a liquid core capsule with an alginate shell around it.

The simplest approach to synthesizing polymeric capsules involves using polyelectrolytes such as alginate. To create a gel-core alginate capsule, we dropped a solution of sodium alginate into a bath containing Ca2+ ions. These ions act to physically crosslink the neighboring alginate chains. After preparing the alginate core capsules, we allowed them to stabilize for 15 minutes before centrifuging them out of the Ca2+ ion bath solution in Figure 2.14. Subsequently, we immersed the capsules in separate solutions of formalin and sulfite buffer, allowing each set of capsule beads to soak for an hour.

Previously, both species, formalin and sulfite mixtures were mixed together in the same capsule, but now each species is contained in its own bead—formalin in one and sulfite mixture in another. As a result, as the formalin and sodium sulfite mixtures diffuse separately from their respective beads into the porous gel system at the most EDC induced shrunken gel, the clock reaction is triggered.

This reaction is observable through a change in pH. The use of capsule beads enhances the reconfiguration of the porous gel in two significant ways. Firstly, it incorporates the clock

reaction with controlled release mechanisms, ensuring a precise timing of chemical interactions. Secondly, it simplifies the reconfiguration into a single-step process, streamlining the overall procedure and improving efficiency.

Although the clock reaction incorporated into the capsule beads in a single-step process does not reswell the porous gels beyond their original 100% volume—as opposed to when it is performed in a two-step process where the clock reaction is inputted by volume—it remains highly effective for allowing controlled release as demonstrated in Figure 2.15.

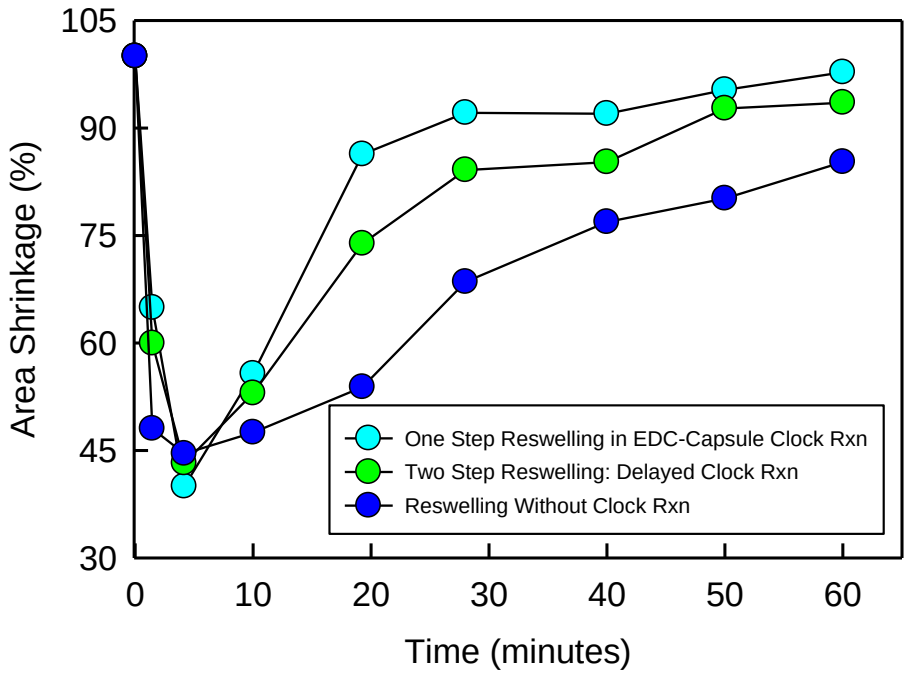

Figure 2.15. Comparison of porous gel reconfiguration processes: a one-step process using MES-(EDC-capsule), a two-step process involving MES-EDC followed by a clock reaction, and a control setup using MES-EDC without a clock reaction.

In our experiments, we tested individual beads containing formalin and sulfite mixtures, alongside several controls: a porous gel in the MES-EDC system without any clock reaction (our initial reswelling strategy) and another control where the capsules were added five minutes after

EDC had induced maximum shrinking. The one-step process involving EDC and the immediate introduction of the clock reaction capsules consistently achieved the highest reswelling percentages after an initial drop, suggesting it might be the most efficient method for reswelling the gel. Following closely was the two-step process with a five-minute delay, confirming that the clock reaction is effectively taking place and allowing the gels to continue reswelling; this indicates that even when the clock reaction is delayed, it still significantly contributes to reswelling. In contrast, setups with only EDC and no clock reaction consistently showed the lowest reswelling percentages, underscoring the crucial role of the clock reaction in enhancing the gel's reswelling efficiency.

2.3.10 Effect of Capsule Size on Gel Reconfiguration

In previous experiments, we manipulated the formalin concentration to tune the transient pH dynamics within the porous gel system. At a formalin concentration of 0.1 M, combined with initial sulfite mixture concentrations of 0.2M sodium metabisulfite and 0.02M sodium sulfite, we observed significant re-swelling of the porous gel system. However, with the current approach of delaying the clock reaction captured in capsule beads, the window during which the pH spikes occur might differ. This is because the species are diffusing out and then mixing within the porous gel at a slower rate. Therefore, it became essential to investigate whether increasing or decreasing concentrations of formalin would have an impact. Indeed, the reswelling of the porous gel is much faster at lower concentration of formalin as indicated.

The set up for this approach was similar we tested individual beads containing formalin and sulfite mixtures at different concentrations. At a 0.1 M formalin concentration, there is a notable surge in reswelling between 10 to 20 minutes, where it almost reaches 70% of the initial reswelling rate, in contrast to the 1.2 M and 3.6 M formalin concentrations which exhibit a more

gradual increase. At the 20-minute interval, the gels with 0.1 M formalin exhibit a much more rapid reswelling compared to those with 1.2 and 3.6 M formalin. Continuing to the 70-minute mark, the reswelling rates for 1.2 M and 3.6 M formalin still show a gradual increment, whereas the reswelling for 0.1 M formalin appears to plateau, suggesting stability in its behavior. The integral clock reaction maintains consistency at a 0.1 M formalin concentration, evident in both beaker and capsule form. Consequently, porous gel systems integrating the clock reaction will utilize the 0.1 M formalin concentration.

To optimize the one-step process of controlled release of the clock reaction in capsules, we varied the size of the capsules, testing diameters of 1.2 cm, 7 mm, and 1 mm. This variation aimed to determine if the size of the capsules affects the speed of the controlled release of clock reaction. The largest beads, with a 1.2 cm diameter, consistently showed the best reswelling performance of the gels compared to the smaller sizes as shown in Figure 2.16.

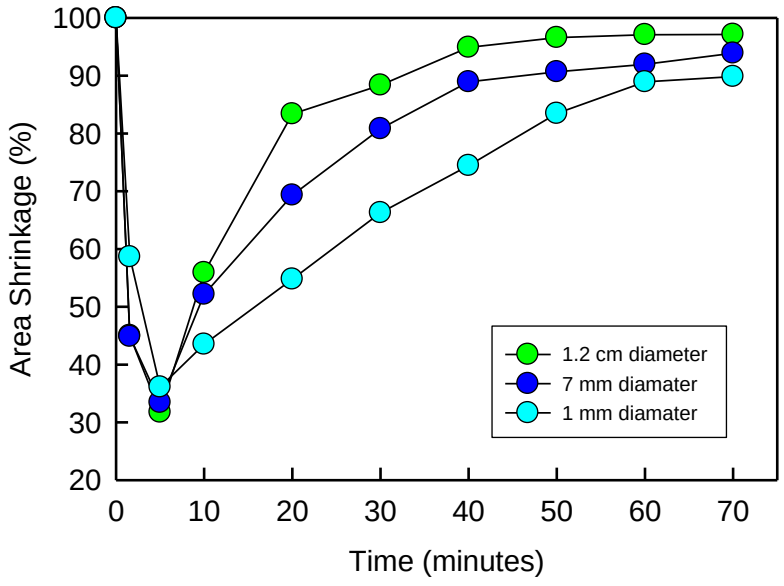

Figure 2.16. Effect of Capsule Size on Gel Reconfiguration. Varying diameter size of capsule beads at 1.2 cm, 7mm, and 1mm.

It was initially hypothesized that the smaller beads (1mm) would release the contents faster due having smaller time scale, suggesting a quicker onset of the clock reaction. However, it appears that the smaller beads might not release a sufficient concentration of the reactants to trigger the clock reaction effectively. In contrast, the larger beads (1.2 cm) released the clock reaction at an optimal rate. Effectively the medium sized capsules fall in between in terms of the release of the clock reaction. However eventually all the capsules sized clock reactions reach about 70% more of the initial swelling. This performance of the largest capsules can be attributed to the fact that all the capsules do not carry the same volume of the clock reaction species. The initial hypothesis suggested that smaller beads (1mm) would release their contents more rapidly, potentially leading to a faster initiation of the clock reaction due to a shorter time scale. However, the results indicated that these smaller beads might not achieve a sufficient concentration of reactants to effectively trigger the clock reaction. In contrast, larger beads (1.2cm) released the reactants at an optimal rate for the clock reaction to occur efficiently. Medium-sized capsules exhibited release rates that fell between those of the smallest and largest beads. Ultimately, regardless of size, all capsule types achieved about 70% more swelling from their initial state. The superior performance of the largest capsules can be attributed to differences in the volume of clock reaction species they carry. For example, to match the volume of reactants in 30 large capsules (1.2cm), the number of smaller capsules (both 7mm and 1mm) would need to be increased fivefold. This insight could be used to refine future experiments, such as adjusting the number of capsules used to ensure consistent reactant volume across different capsule sizes, thereby optimizing the experimental setup.

2.4 Conclusions

To expedite the reconfiguration of the existing MES-EDC porous gel system, we proposed a secondary reaction that increased the solution pH five minutes after adding EDC. This timing ensures maximal contraction of the hydrogel before triggering the secondary reaction.

Adding a highly alkaline solution allows the hydrogel to expand more rapidly than with the MES-EDC-only reaction network. This approach not only shortened the re-swelling time to less than 15 minutes but also expanded the gel beyond its initial size by an additional 20%. The formalin-sulfite clock reaction, introduced as a secondary reaction cycle, didn't match the rate of NaOH-induced reconfiguration but significantly enhanced re-swelling. Even 15 minutes post maximum contraction, the gels exhibited an expansion approximately 20% greater than without the clock reaction.

At the lowest formalin concentration of 0.1 M, the porous hydrogel showed the most substantial swelling, reaching nearly 200% after 60 minutes. Lower formalin concentrations preserve more carboxyl groups' functionality, crucial for re-swelling percentages, highlighting the clock reaction's crucial role in enhancing reswelling higher formalin concentrations led to more extensive crosslinking, reducing free carboxyl groups and likely increasing anhydride bonds, slowing hydrolysis, and resulting in less swelling.

To maintain the autonomous shape configuration of the hydrogel, we aim to introduce all chemicals simultaneously. The formalin-sulfite clock reaction, where formaldehyde reacts with bisulfite ions to increase pH, is suggested to accelerate reconfiguration. Integration of this reaction cycle into the porous gel results in faster reconfiguration period (15 minutes) and a 20% increase in initial expansion compared to the MES-EDC network alone. Lower formalin

concentrations promote significant swelling by preserving carboxyl groups' functionality, crucial for water absorption and hydrolysis of anhydride bonds. Conversely, higher formalin concentrations lead to less swelling due to increased crosslinking and slower hydrolysis. Incorporating the clock reaction in capsule beads streamlines the process into a single-step re-swelling. Even with a delayed clock reaction, significant reswelling occurs with capsule beads.

Chapter 3: Summary and Future Experiments

3.1 Key Findings

Firstly, it was observed that the 1:3 porous gels exhibited the least contraction (~60%) but the fastest recovery, with more than 90% of the gel area recovered within the first 20 minutes. In contrast, both the 3:1 and 1:1 gels showed similar levels of contraction (30-40%), with the 3:1 gels slightly outperforming the 1:1 gels in terms of shrinkage. The differing behavior among the gels can be attributed to variations in Aac concentration, with the 1:3 gel containing the least amount of Aac, resulting in fewer anhydride bonds and consequently less shrinkage.

Beyond 1 equiv. of EDC, the gels reached a quasi-steady state, maintaining their shrunken size until all fuel was consumed. This stabilized state was facilitated by excess EDC, ensuring the conversion of all carboxylates to anhydrides. The rate of contraction or expansion was then governed by the slower hydrolysis of anhydrides, with higher concentrations of EDC leading to prolonged contracted states.

Furthermore, the incorporation of a highly alkaline (NaOH) solution allowed for more rapid expansion of the porous hydrogel, surpassing the efficiency of the MES-EDC network alone. This enhancement was attributed to the increased pH, facilitating faster anhydride hydrolysis and autonomous reswelling.

The introduction of the formalin-sulfite clock reaction provided a potential approach to autonomously accelerate the reconfiguration rate of porous gels. While not matching the rate of NaOH-induced reconfiguration, the clock reaction significantly contributed to increased re-swelling, indicating its effectiveness in accelerating anhydride hydrolysis. In optimizing the conditions for the clock reaction, varying the initial concentration of formalin proved to be more

influential than aging the formalin solution. Lower formalin concentrations facilitated rapid pH increase and extensive hydrolysis, resulting in significant swelling of the porous gels. Ultimately, the formalin-sulfite clock reaction, where formaldehyde reacts with bisulfite ions to increase pH, is suggested to accelerate reconfiguration. Integration of this reaction cycle into the porous gel results in faster reconfiguration period (15 minutes) and a 20% increase in initial expansion compared to the MES-EDC network alone.

Additionally, incorporating the clock reaction into capsule beads simplified the reconfiguration process into a single-step procedure, improving efficiency and controlled release. This approach addressed two major issues: 1) the slow response time of hydrogels, and 2) the automation of external stimuli, such as pH changes induced by the clock reaction, in the reconfiguration cycle of porous gels.

3.2 Integration of Clock Reaction on Hybrid Porous Gel Reconfiguration

The exploration of different acrylic acid to acrylamide monomer ratios led to the development of a hybrid gel. This gel is composed of two distinct segments, each with its own monomer ratio, seamlessly connected in the middle to form a single integrated structure. On one side of the gel, the acrylic acid to monomer ratio is 3:1, while on the other, it is 1:1. The interface where these two ratios meet is centrally located within the gel. This unique configuration was achieved during the foaming process that preceded polymerization. The two gel components were foamed adjacent to each other, with the 3:1 ratio positioned on the left side and the 1:1 ratio on the right, allowing them to merge at the center as shown in Figure 3.1. This arrangement facilitates distinct properties on either side of the hybrid gel, tailored by their respective monomer concentrations.

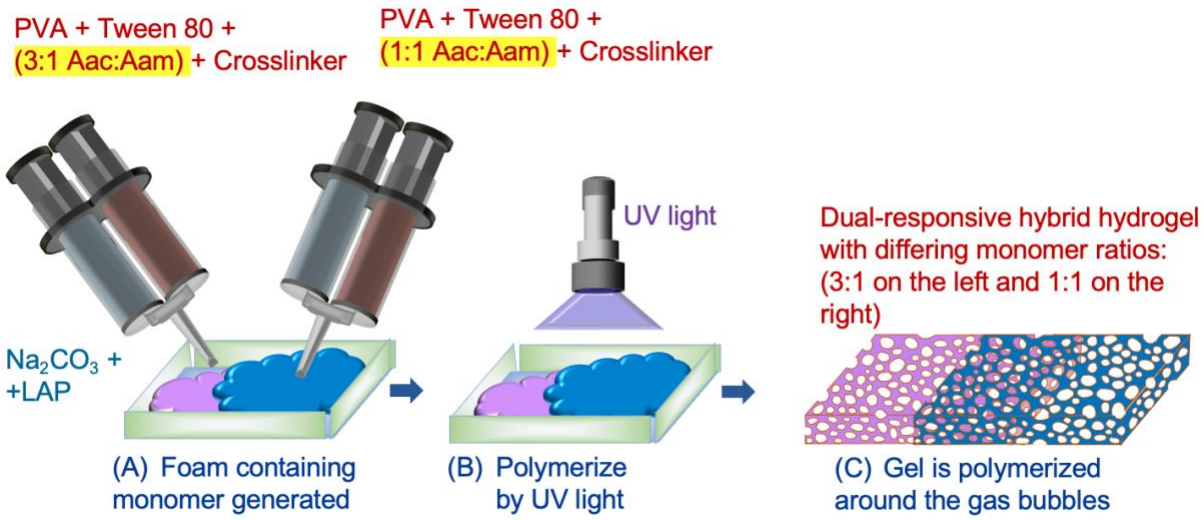

Figure 3.1. Synthesis of hybrid gel. Hybrid gel with dual responsive characteristic as shown with differing monomer ratios (left being 3:1 and right being 1:1).

This hybrid gel features an interface that connects two types of gels: on the left-hand side, the ratio is acrylic 3:1, and on the right, it is 1:1.

In our future experiment, maintaining the integrity of the clock reaction will be crucial as we plan to test it using a hybrid gel. This gel, which will be a combination of two different monomer ratios, is expected to double the mass and volume compared to the initial gel, potentially complicating the clock reaction. To address these complexities, we will simplify the process by doubling the initial swelling volume of MES while keeping the amount of EDC consistent with the equivalent required for the combined ratios of the two gels. Furthermore, we will adjust the system by increasing the number of capsules from 30 to 60, dividing them evenly between formalin and sulfite mixtures, ensuring that the reaction's parameters are maintained despite the gel's increased scale. These gels will show integration with the clock reaction.

This hybrid gel is expected to feature distinct shrinking and reswelling properties, making it suitable for a variety of applications including drug delivery, tissue engineering, soft robotics, and agriculture. Moreover, its versatility will be enhanced by the ability to fine-tune the

reswelling behavior through variations in monomer concentrations, enabling tailored functionality for specific needs.

Bibliography

[1] Boekhoven, J.; Brizard, Aurelie M.; Kowlgi, Krishna N. K.; Koper, Ger J. M.; Eelkema, R.; van Esch, Jan H. Dissipative Self-Assembly of a Molecular Gelator by Using a Chemical Fuel. *Angewandte Chemie International Edition* **2010**, *49* (28), 4825–4828.

[2] De, S.; Rafał Klajn. Dissipative Self-Assembly Driven by the Consumption of Chemical Fuels. *Advanced Materials* **2018**, *30* (41).

[3] Horio, T.; Murata, T. The Role of Dynamic Instability in Microtubule Organization. *Frontiers in Plant Science* **2014**, *5*.

[4] Merindol, R.; Walther, A. Materials Learning from Life: Concepts for Active, Adaptive and Autonomous Molecular Systems. *Chemical Society Reviews* **2017**, *46* (18), 5588–5619.

[5] Bermudez, J. G.; Deiters, A.; Good, M. C. Patterning Microtubule Network Organization Reshapes Cell-like Compartments. *ACS synthetic biology* **2021**, *10* (6), 1338–1350.

[6] Bera, A.; Gupta, M. L. Microtubules in Microorganisms: How Tubulin Isotypes Contribute to Diverse Cytoskeletal Functions. *Frontiers in Cell and Developmental Biology* **2022**, *10*.

[7] Marcin Fiałkowski; Kyle; Rafal Klajn; Smoukov, S. K.; Campbell, C. S.; Grzybowski, B. A. Principles and Implementations of Dissipative (Dynamic) Self-Assembly. *Journal of Physical Chemistry B* **2006**, *110* (6), 2482–2496.

[8] San Antonio, J. D.; Jacenko, O.; Fertala, A.; Orgel, J. P. R. O. Collagen Structure-Function Mapping Informs Applications for Regenerative Medicine. *Bioengineering* **2021**, *8* (1), 3.

[9] Svitkina, T. The Actin Cytoskeleton and Actin-Based Motility. *Cold Spring Harbor Perspectives in Biology* **2018**, *10* (1), a018267.

[10] Fujiwara, I.; Takeda, S.; Oda, T.; Honda, H.; Narita, A.; Maéda, Y. Polymerization and Depolymerization of Actin with Nucleotide States at Filament Ends. *Biophysical Reviews* **2018**, *10* (6), 1513–1519.

[11] Clamons, S.; Qian, L.; Winfree, E. Programming and Simulating Chemical Reaction Networks on a Surface. *Journal of The Royal Society Interface* **2020**, *17* (166), 20190790.

[12] Irving, M. Regulation of Contraction by the Thick Filaments in Skeletal Muscle. *Biophysical Journal* **2017**, *113* (12), 2579–2594.

[13] Ho, T.-C.; Chang, C.-C.; Chan, H.-P.; Chung, T.-W.; Shu, C.-W.; Chuang, K.-P.; Duh, T.-H.; Yang, M.-H.; Tyan, Y.-C. Hydrogels: Properties and Applications in Biomedicine. *Molecules* **2022**, *27* (9), 2902.

[14] Rizwan, M.; Yahya, R.; Hassan, A.; Yar, M.; Azzahari, A. D.; Selvanathan, V.; Sonsudin, F.; Abouloula, C. N. PH Sensitive Hydrogels in Drug Delivery: Brief History, Properties, Swelling, and Release Mechanism, Material Selection and Applications. *Polymers* **2017**, *9* (4), 137.

[15] Zhou, Y.; Jin, L. Mechanics Underpinning Phase Separation of Hydrogels. *Macromolecules* **2023**, *56* (2), 426–439.

[16] Palanivelu, S. D.; Armir, N. A. Z.; Zulkifli, A.; Hair, A. H. A.; Salleh, K. M.; Lindsey, K.; Che-Othman, M. H.; Zakaria, S. Hydrogel Application in Urban Farming: Potentials and Limitations—a Review. *Polymers* **2022**, *14* (13), 2590.

[17] Cao, H.; Duan, L.; Zhang, Y.; Cao, J.; Zhang, K. Current Hydrogel Advances in Physicochemical and Biological Response-Driven Biomedical Application Diversity. *Signal Transduction and Targeted Therapy* **2021**, *6* (1), 1–31.

[18] Choudhary, H.; Raghavan, S. R. Superfast-Expanding Porous Hydrogels: Pushing New Frontiers in Converting Chemical Potential into Useful Mechanical Work. *ACS Applied Materials & Interfaces* **2022**, *14* (11), 13733–13742.

[19] Udaykumar Vegad; Patel, M.; Dignesh Khunt; Ožbej Zupančič; Chauhan, S.; Amrit Paudel. PH Stimuli-Responsive Hydrogels from Non-Cellulosic Biopolymers for Drug Delivery. *Frontiers in bioengineering and biotechnology* **2023**, *11*.

[20] Xing, Y.; Zeng, B.; Yang, W. Light Responsive Hydrogels for Controlled Drug Delivery. *Frontiers in Bioengineering and Biotechnology* **2022**, *10*.

[21] Kasiński, A.; Zielińska-Pisklak, M.; Oledzka, E.; Sobczak, M. Smart Hydrogels – Synthetic Stimuli-Responsive Antitumor Drug Release Systems. *International Journal of Nanomedicine* **2020**, *Volume 15*, 4541–4572.

[22] Liu, J.; Huang, Y.-S.; Liu, Y.; Zhang, D.; Kaloian Koynov; Butt, H.-J.; Wu, S. Reconfiguring Hydrogel Assemblies Using a Photocontrolled Metallopolymer Adhesive for Multiple Customized Functions. *Nature chemistry* **2024**.

[23] Klouda, L.; Mikos, A. G. Thermoresponsive Hydrogels in Biomedical Applications. *European Journal of Pharmaceutics and Biopharmaceutics* **2008**, *68* (1), 34–45.

[24] Chen, X.; Stasi, M.; Jennifer Rodon Fores; Großmann, P. F.; Bergmann, A. M.; Dai Keino; Tena-Solsona, M.; Rieger, B.; Job Boekhoven. A Carbodiimide-Fueled Reaction Cycle That Forms Transient 5(4*H*)-Oxazolones. *Journal of the American Chemical Society* **2023**, *145* (12), 6880–6887.

[25] Morell, M.; Puiggalí, J. Hybrid Block Copolymers Constituted by Peptides and Synthetic Polymers: An Overview of Synthetic Approaches, Supramolecular Behavior and Potential Applications. *Polymers* **2013**, *5* (1), 188–224.

[26] Chen, X.; Würbser, M. A.; Job Boekhoven. Chemically Fueled Supramolecular Materials. *Accounts of materials research* **2023**, *4* (5), 416–426.

[27] Dodo, O. J.; Petit, L.; Chamoni W. H. Rajawasam; C. Scott Hartley; Dominik Konkolewicz. Tailoring Lifetimes and Properties of Carbodiimide-Fueled Covalently Cross-Linked Polymer Networks. *Macromolecules* **2021**, *54* (21), 9860–9867.

[28] Heckel, J.; Loescher, S.; Mathers, R. T.; Walther, A. Chemically Fueled Volume Phase Transition of Polyacid Microgels. *Angewandte Chemie* **2021**, *60* (13), 7117–7125.

[29] Kovacs, K.; McIlwaine, R.; Gannon, K.; Taylor; Scott, S. K. Complex Behavior in the Formaldehyde−Sulfite Reaction.*The journal of physical chemistry. A.* **2004**, *109* (1), 283–288.

[30] Fletcher, D. A.; Mullins, R. D. Cell Mechanics and the Cytoskeleton. *Nature* **2010**, *463* (7280), 485–492.

[31] Schneider, F.; Metz, I.; Rust, M. B. Regulation of Actin Filament Assembly and Disassembly in Growth Cone Motility and Axon Guidance. *Brain Research Bulletin* **2023**, *192*, 21–35.

[32] Sakamoto, R.; Murrell, M. P. F-Actin Architecture Determines the Conversion of Chemical Energy into Mechanical Work. *Nature communications* **2024**, *15* (1).